IMPROVING URBAN AIR AND STORMWATER QUALITY USING PHOTOCATALYTIC HIGHWAY PAVEMENT AND PHOTOCATALYTIC PERVIOUS CONCRETE SHOULDERS

A THESIS IN
Civil Engineering

Presented to the Faculty of the University
of Missouri-Kansas City in partial fulfillment of
the requirements for the degree

MASTER OF SCIENCE

by
FERAS EL-GHUSSEIN

B.S., University of Missouri-Kansas City, 2010

Kansas City, Missouri
2013

IMPROVING URBAN AIR AND STORMWATER QUALITY USING PHOTOCATALYTIC HIGHWAY PAVEMENT AND PHOTOCATALYTIC PERVIOUS CONCRETE SHOULDERS

Feras El-Ghussein, Candidate for the Master of Science Degree

University of Missouri-Kansas City, 2013

ABSTRACT

Pervious concrete, photocatalytic concrete, and photocatalytic pervious concrete are emerging technologies in the pavement industry, and have been researched in order to determine the efficacy of these technologies in environmental sustainability on a wide scale. In this thesis, the effects of photocatalytically active cement on a highway were studied, along with the affects of photocatalytic pervious and conventional pervious concrete shoulders. A laboratory experimental setup was conducted simultaneously as a comparison between theoretical and practical implementations of this technology. The results of the laboratory test indicated that there was not a significant increase in nitrate, but the nitrite levels increased significantly. This could be indicative of the rolls humidity and total sunlight play in the reactivity of the photocatalytic concrete, but needs further assessment for conformation. It may also suggest the role of retention time of the water within the pervious

concrete as well. The field results indicate that nitrate levels were present early on in the construction phase of the project, even prior to opening the highway to the public and to large traffic volumes. Data indicates that the base was drainable and drained quickly, despite the amount of fines within subbase. It was also determined that water had an effect on the temperature of the pavements, as heat was drawn away from the subbase during rain events. Further data needs to be collected and analyzed in order to more certainly determine effect of this technology on water quality. Further assessment need also be conducted on the use of pervious concrete as highway shoulders. This was suspected to be the first highway pavement in the world in which photocatalytically active cements were utilized for air and water quality improvements, and it is also suspected to be the first highway in which pervious concrete shoulders were used for stormwater management.

The faculty listed below, appointed by the Dean of the school of Computing and Engineering, have examined a thesis titled “Improving Urban Air and Stormwater Quality Using Photocatalytic Highway Pavement and Photocatalytic Pervious Concrete Shoulders," presented by Feras El-Ghussein, candidate for the Masters of Science degree, and certify that in their opinion it is worthy of acceptance.

Supervisory Committee

John Kevern, Ph.D., Committee Chair
Department of Civil Engineering

Ceki Halmen, Ph.D.
Department of Civil Engineering

Deborah O’Bannon, Ph.D.
Department of Civil Engineering

CONTENTS

LIST OF ILLUSTRATIONS

LIST OF TABLES

ACKNOWLEDGMENTS

I would like to begin by thanking my parents for all that they have done for me throughout my whole life. My mom and dad have provided me with support in the most amazing ways; through their thoughts and prayers, their advice, their pride in my siblings and I, and their simple guidance to keep me on my toes at all times. As immigrants, they always were cautious for me, which kept me out of trouble on more occasions than I can count, and they always wanted me to excel, which kept me wanting to strive and achieve what seems impossible. Without them, I would not be who I am today, and for this and for how awesome they are, I thank and love them greatly. I would also like to acknowledge and thank my loving brother and sister, who have given me more of their time then I may even deserve. Despite any sibling rivalry, they were always there when I needed them, which is more than what I can say about myself with respect to them. I would like to certainly acknowledge with love and affection my niece Zaina and my nephew Omar, who were too young to remember their father who was killed by a drunk driver. Trying to be a role model and a father figure to them was more challenging than any thesis or masters degree, and I hope that I will be successful in helping to raise and rear them to be the best that they can be. Last, but certainly not least, I would like to acknowledge my beloved wife, who encouraged me from the very start to succeed, even if it meant we were not with each other as often as we would like to be. Along with thanking my family, I would also like to apologize to them as well. I have always attempted to be the best son, the best brother, the best friend, and the best husband, but more often than not, I would be too occupied to even recognize their needs immediately. If I had

ever shown any shortcomings of any sort, than please forgive me, and know it was unintentional. I love you more than I can put into words.

I would also like to send special regards to my advisor, Dr. John Kevern, who has given me more than just academic advice, but rather a chance to participate in a wonderful project, as well as a chance to learn more than I could have dreamed of in the last few years. I also send my regards to the rest of the faculty and staff at UMKC who have helped me in completing my masters. There are many people that have helped me in completing my degree and helped me stand out in life; to all of them, it seems too small, but Thank You!

CHAPTER 1

INTRODUCTION

Pervious concrete is used to manage stormwater runoff, and is typically used in low volume roads and parking lots. In a project to test pervious concrete characteristics in a high volume arterial road, two sections of the shoulder of a Missouri highway near St. Louis, Missouri were paved with pervious concrete. The test section was approximately 1200 feet long, and both the pervious concrete and the mainline pavement were paved using a photocatalytically active cement concrete marketed under the trade name 'TX Active'. The control section was also approximately 1200 feet long, and both the pervious concrete and the mainline pavement were paved using ordinary Portland cement. Photocatalytically active cement reacts with contaminates on the surface of the concrete as well as in air in contact with the concrete to reduce pollutants. This process is catalyzed by the presence of ultraviolet radiation from the sun. In order to determine the feasibility and advantages of using pervious concrete and photocatalytically active cements in highways, testing included materials testing of the concrete and the subbase, water quantity measurements to measure the volume of rainwater runoff from the mainline as well as the shoulders, water quality measurements to determine the efficacy of both the pervious and the TX Active concretes, air quality

measurements (completed by another project team) to determine air pollution reduction from the TX Active concrete, and other concrete profile measurements to determine the overall impact of/on the highway and shoulders.

This report documents the phases of the highway construction including pre/post-construction findings, instrumentation and test methods, pertinent construction obstacles that have altered the preliminary arrangements, all of the aforementioned test results excluding air quality analysis, and laboratory testing to compensate for missing or invalid data. The report is setup in the following manner:

- Chapter 2: A synopsis of the studies and journal articles summarizing all of the prevalent technologies used in the highway pavement is provided in chapter 2.
- Chapter 3: Methods and instrumentation used for the analysis of the results are discussed in this chapter, along with standards and specifications used in this endeavor and any alteration to these known methods.
- Chapter 4: The laboratory study is provided in this chapter, along with exact chronological order of experimentation, observations made, and results of the laboratory testing.
- Chapter 5: The construction procedure is discussed in chapter 5, along with figures of the processes of constructing the highway and placing field instruments and apparatuses.
- Chapter 6: The data and results that were determined in the field are provided within this chapter.

- Chapter 7: The construction challenges are explained in this chapter, along with possible causes to some system malfunctions. Also discussed are the best practices for future endeavors and the lessons learned from this project.
- Chapter 8: The data and results are summarized and discussed in this final chapter, along with the conclusions that were observed.

Background Information

The section of highway being researched is Missouri Highway 141in Chesterfield, Missouri between Olive Boulevard and Ladue Road. The highway travels north-south, but the researched portion is in the southbound lanes. The owner of the highway is the Missouri Department of Transportation (MoDOT), and the contractor that constructed the highway is Fred Weber, Inc. The total length of photocatalytic pavement was approximately 1200 feet, and the total length of photocatalytic pervious concrete was approximately 75 feet. The photocatalytic pavement was constructed in two-lifts, as opposed to typical one-lift pavement. The total length of the effective conventional concrete zone was similarly 1200 feet, and the conventional pervious concrete was approximately 75 feet as well. The control pervious and the photocatalytic pervious shoulders utilized internal curing to in place of plastic curing. After completion, the highway was opened to the public and can serve more than 50,000 cars per day (Shapiro 2012).

Testing Objectives

The objective of this study was to determine the efficacy of pervious concrete and photocatalytic concrete in highway pavements. This was done in two ways; a laboratory

simulation of the highway pervious concrete shoulders and field testing on the highway. The laboratory simulation was meant to provide baseline data for water quality analysis purposes, as well as verify expected trends associated with the reactivity of the photocatalytic material. The field testing was meant to provide the actual values of water quality improvements due to the pervious concrete/photocatalytic concrete, the water quantity values to determine the efficacy of the permeable pavements, and temperature profiles of the differing pavements.

CHAPTER 2

LITERATURE REVIEW

Photocatalysis of Titanium Dioxide

Titanium dioxide (TiO_2) is a semiconductor which is activated by ultraviolet light radiation and oxidizes/reduces pollutants. This process is called heterogeneous photocatalysis, and can also be achieved with other semiconductors (Dylla et al. 2011). TiO_2 oxidizes adsorbed water and other hydroxyl groups and forms radical hydroxides as shown in the following equations:

$$h_{tr}^{+} + H_2O \rightarrow H^{+} + OH*$$
$$h_{tr}^{+} + OH^{-} \rightarrow OH*$$

where h_{tr}^{+} is a trapped electron hole on the surface of the TiO_2. Reactive oxygen species and superoxides can be formed by TiO_2 as shown in the following equations:

$$e_{tr+}^{-} + O_2 \rightarrow O_2{}^{*-}$$
$$O_2{}^{*-} + H_3O^{+} \rightarrow HO_2* + H_2O$$
$$2HO_2* \rightarrow H_2O_2 + O_2$$
$$e_{tr+}^{-} + H_2O_2 \rightarrow OH* + OH^{-}$$

where e_{tr}^- is a trapped electron (Zhang et al. 2009). These radical hydroxides and superoxides in turn react with pollutants such as nitrogen oxides (Fujishima et al. 2005). The pollutants are transformed into nonhazardous materials with little energy consumption and little selectivity of decomposition (Dylla et al. 2011). In the case of TiO_2, a secondary reaction occurs due to the photo-induced superhydrophilicity. In other words, the presence of water removes particulates that have reacted with the TiO_2, allowing TiO_2 treated surfaces to be 'self-cleaning'. Other materials can be used to achieve this superhydrophilicity, but it is worth noting that TiO_2 is unique in the fact that it undergoes these two separate, unrelated reactions in the presence of light radiation (Fujishima et al. 2005).

Photocatalytic Concrete

Research has shown that using the photocatalytic agents can reduce the levels of nitrogen oxides (NO_x) in the ambient environment, and with over half of NO_x being produced by mobile sources such as traffic emissions, efforts have been made to mitigate these emissions using TiO_2 (Dylla et al. 2011). In the presence of TiO_2, the NO_x gasses, nitric oxide (NO) and nitrogen dioxide (NO_2) react to produce nitrate ions (NO_3^-), which washes away in the presence of water, as shown in Figure 1 (Dylla et al. 2011).

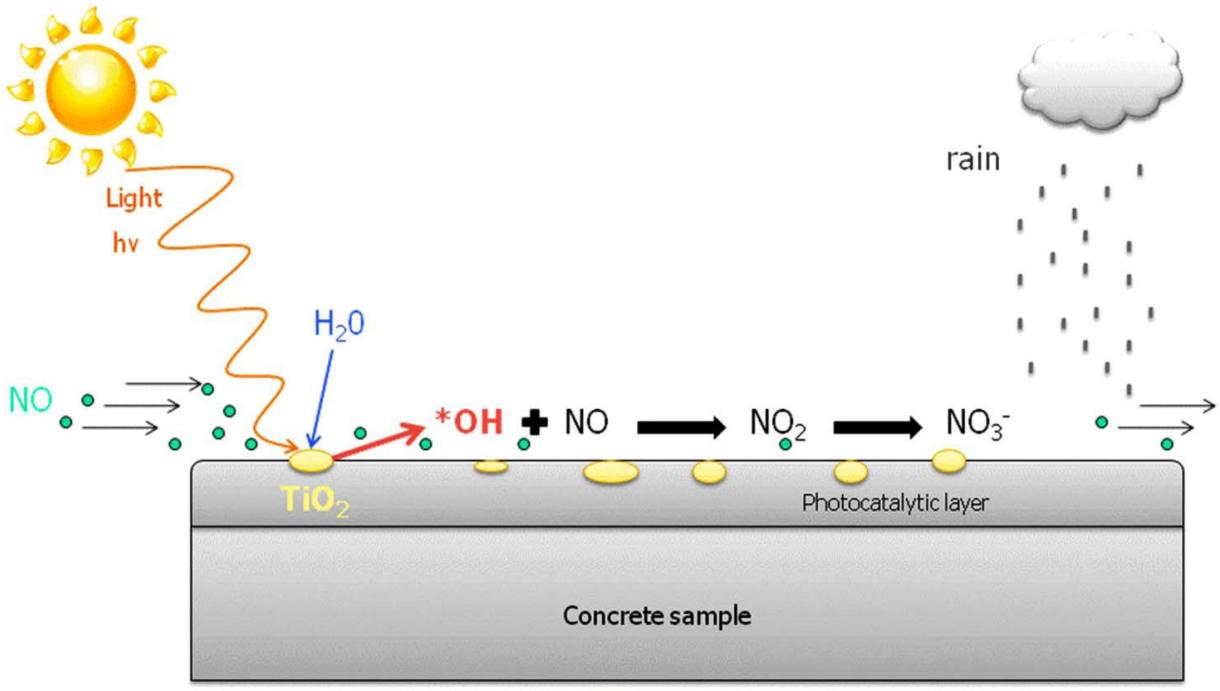

Figure 1. Photocatalytic oxidation of NO and NO_2 by concrete pavement containing TiO_2 (Dylla et al. 2011)

By knowing the total amount of NO_x within the atmosphere and the total NO_x after the ambient conditions have reached equilibrium, the total efficacy of the TX Active cements can be determined (Hasan et al. 2010). Figure 2 shows the reduction of NO_x due to the TX Active cements in a laboratory test (Dylla et al. 2011).

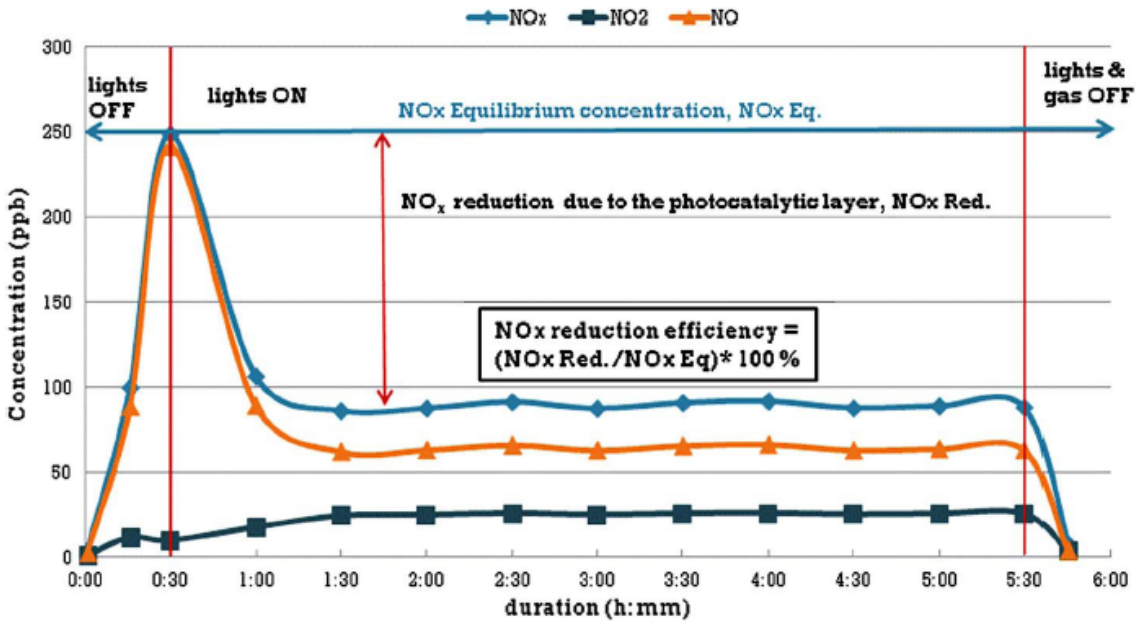

Figure 2. Reduction in NOx due to TX Active Concrete (Dylla et al. 2011)

Different application methods of TiO_2 on pavements have been evaluated to determine environmental benefits as well as the affect of TiO_2 on durability of pavements. These methods included concrete blocks with the surfaces coated with a cement and TiO_2 paste, 'a cementitious-based ultrathin coating' on a concrete pavement surface, a water based treatment applied using a spray gun, and a sprinkling treatment where TiO_2 nanoparticles were sprinkled on a fresh concrete surface (Dylla et al. 2011). The results of testing conducted on the latter three indicated that the most efficient methods were the cement-based and the water-based applications. The cement-based application, however, was more susceptible to abrasion, yet still leading the nitrogen oxide removal efficiency (Hassan et al. 2010). Other testing indicated that TiO_2 particles were inert during hydration (did not react

with hydration products), although the nano-sized particles did seem to accelerate hydration and improve the early age degree of hydration. As a result of the improved hydration, porosity decreased, the pore size distribution had also been altered, and the compressive strength increased. Due to the surface area of the nano-sized particles, the water demand was increased in order to obtain consistency of the mix (Chen et al. 2012).

Other studies have also observed the environmental loading conditions on photocatalytic pavements by mimicking real world scenarios. This included applying typical roadway contaminates including silty-clay type soils, deicing salts, and motor oil. The testing concluded that the three contaminate types reduced the NO_x removal efficiency, with the worst being the motor oil. Furthermore, this study had determined that the increased flow rate of contaminates reduced the efficiency of NO_x removal, as did the increase of relative humidity. A similar study had determined that higher ratios of nitrogen dioxide to nitrogen oxides (NO_2/NO_x) decreased the efficiency of NO_x removal, but this was dependant on other factors such as flow rate of contaminate applications and humidity. This study had also determined that the highest reactivity was achieved at 25% relative humidity (Dylla et al. 2011).

Pervious Concrete Pavements

Pervious concrete allows for water infiltration as shown in Figure 3 (Purintion Builders 2010). Similar to conventional concrete pavements, Portland cement pervious concrete (PCPC) is a concrete composed of cement, water, and aggregate, and is typically placed on an aggregate subbase; however, PCPC has little to no fine aggregate, and has a

series of voids which give the concrete its perviousness (Michigan Concrete Association 2006).

Figure 3. Water infiltration into a pervious concrete surface (Purintion Builders 2010)

The aggregate subbase along with the pavement itself acts as a mechanical filter and a detention basin, and thus controls pollution entering into streams and waterways. Additionally, hydrocarbons seeping from vehicles attach to the large surface area of the pervious concrete or within the aggregate subbase, and degrade naturally, further improving the water quality from pervious concrete (Asadi et al. 2012). As the subbase retains water and allows percolation into soils, another advantage of PCPC is the replenishment of water aquifers beneath the pavement. Another advantage of PCPC is the fact that it has the

potential of replacing other stormwater management systems, since it acts as a pavement, retains water, and improves water quality. This, in turn, allows for greater utilization of land and greater economic benefits, as standalone systems need not be built and maintained. Yet another environmental advantage of PCPC is the reduction of the urban heat island effect, a phenomenon where materials with darker color and lower albedo absorb and store heat. This reduction is introduced by the fact that the open system allows the cooler air from the subgrade to cool the PCPC, preventing heat from being stored within the pavement. Along with all of the environmental and economic benefits, PCPC also offers a safer pavement than the conventional pavements for vehicular traffic, as it reduces hydroplaning and eliminates ice formation on the surface (Michigan Concrete Association 2006). It has also been indicated that pervious concrete may be more slip resistant than traditional concretes for pedestrians, and thus may be recommended for areas of high pedestrian traffic with elevated risks of slipping (King et al. 2013).

The greatest factor affecting PCPC durability is construction related practices. The durability and strength of the PCPC are dictated by the design void content, which is produced at a given unit weight. Thus, the void content is achieved by compaction, and over- or under-compaction produce unwanted results (Kevern et al. 2012).

Photocatalytic Pervious Concrete

The higher surface area of pervious concrete (nearly six times greater than impervious concrete) increases photocatalysis, as there is a higher area exposed to sunlight (Asadi et al. 2012). It was reported from a study that the reduction efficiency of NO_x increased with the

depth of the photocatalytic pervious concrete and the ultraviolet light intensity, and the removal efficiency decreased with the increase in pollutant flow rates (Asadi et al. 2012). Photocatalytic pervious concrete was shown to reduce NOx from ambient air, and it was determined that the concentrations deposited on the surface were not high enough to produce undesirable results (Hasan et al. 2011).

Two-Lift Pavements

Two-lift paving is accomplished by paving a bottom lift of a thickness greater than two inches, consisting of a lower quality concrete and containing less cementitious material. The aggregate in the bottom lift is not required to have a high durability, and thus maybe recycled, low quality, and/or cheaper aggregate. Atop of the bottom lift is the premium concrete surface exposed to vehicle traffic and environmental loading, which is placed immediately after the bottom lift is placed and before the bottom lift sets. The top lift typically is approximately two inches thick, contains a high quality aggregate, and has a high durability and a high cementitious material content (Hall, 2007). By using less cement and recycled aggregate in the bottom lift, cost reductions could potentially justify the use of two-lift pavement, while the top lift maintains durability and pavement performance (Cable et al. 2004). An example of two lift pavement is provided in Figure 4, from the construction of this project.

Figure 4. Two-lift pavement and the distinct top and bottom lifts

Two-Lift Construction Examples

Two-lift paving has been practiced in the EU on a large scale. Specifically, the countries of Germany and Austria have had much experience with two-lift paving due to stringent recycling requirements, as well as safety issues arising from friction due to abrupt climate changes (Cable et al. 2004). Other EU nations that have experience in two-lift paving include France, Belgium, and the Netherlands, all with varying degrees of success (Hall, 2007). In France, the need to construct a two-lift pavement arose from the cost of hauling higher quality aggregate that provided higher durability and greater noise reduction. Thus the cost of hauling these materials justified the greater cost of two-lift construction, as the lower quality aggregate for the bottom layer was available locally (Cable et al. 2004).

Two-lift concrete has been used in the US since 1891, however with new requirements necessitating more stringent quality control in pavements; two-lift concrete has seen intermittent usage (Tompkins et al. 2009). During the mid-20th century, requirements for wire mesh reinforcement produced two-lift pavements as two homogenous concrete slabs

placed wet on wet after the wire mesh has been placed atop of the bottom lift. However, this pavement technique has receded until federal scanning programs have identified the use of heterogeneous two-lift pavements in Europe. These programs initiated the construction of two test sections of two-lift pavement, one in the state of Michigan and one in the state of Kansas (Tompkins et al. 2009). Other locations in the US that have used two-lift concrete pavements include Iowa and Florida. Both of these sections are serviceable to date (Cable et al. 2004).

Internal Curing of Concrete

In order to achieve desirable results of concrete surfaces, the concrete must be adequately cured for a certain amount of time. Furthermore, the hydration process ceases once relative humidity is below approximately 80%, so curing is required to maintain the moisture above this threshold (Mindess et al. 2002). Traditionally, curing is completed by keeping the surface moist using one of many possible techniques. However, this can be insufficient as the moisture from external curing may only penetrate a few millimeters of the surface, and not reach the bulk of the concrete (Bentz et al. 2010). This can be mitigated by the process of internal curing, a phenomenon in which absorptive materials give off the moisture withheld from the mixture water once the concrete setting has commenced, as shown in Figure 5 (Bentz et al. 2010). This process, though observed from concretes well over a century old, has only recently been documented.

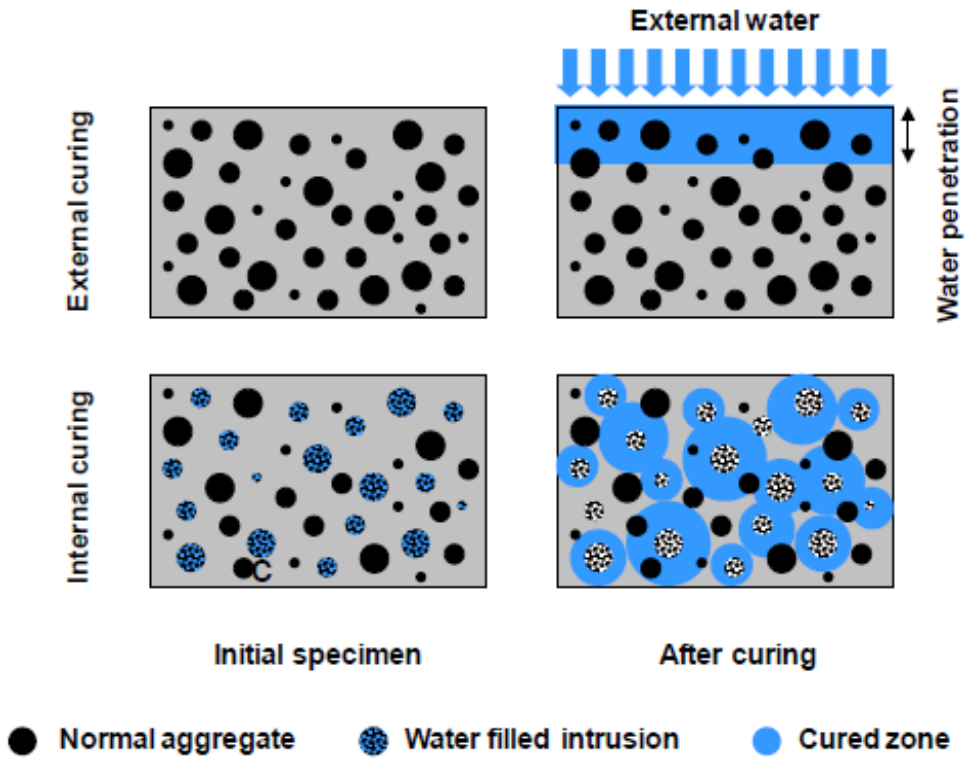

Figure 5. Internal VS. external curing in concrete and the effective area of each (Bentz et al. 2010)

Curing of Concrete

The curing of concrete is the maintenance of sufficient moisture and adequate temperature within the concrete for a suitable period of time after placing and finishing (Mindess et al. 2002). Traditionally, moisture has been introduced to the concrete surface using misters, foggers, burlap blankets, plastic sheeting, or even ponding. All of these techniques are considered external curing (EC) techniques, since only the surface is affected, and are chosen based on preference, availability, need, and simplicity of application. Internal

curing (IC), however, is achieved by introducing moisture from pre-wetted aggregates or other absorptive materials along with the mix water (Kosmatka et al. 2003). This creates a series of pockets filled with water, and these pockets release the moisture once void pressure develops due to chemical shrinkage (Weiss 2012). This water does not increase the water-to-cementitious material ratio, as the concrete must have already set for chemical shrinkage to take place and for these voids to form. Thus, theoretically, this water is strictly used in the curing of the concrete.

EC introduces water to the surface to cure the concrete, and though this water may penetrate a few millimeters of the surface, the bulk of the material has lower moisture than required for curing. IC, on the other hand, disperses water throughout the concrete. From this, it is apparent that IC is more inclusive than EC. Furthermore, IC is not meant to replace EC, it is meant to work alongside it for the most adequate curing possible.

History of Internally Cured Concretes

Lightweight aggregates (LWA) typically produce some IC, even if minimal absorption is available. Natural LWA were used in concretes since the Roman era, including the construction of the dome of the Pantheon in Rome. However, the early 20th century saw an introduction of artificial LWA after the development of a new firing technique in the production of clay, shale, and slate rocks, credited to Stephen Hayde. These aggregates were used in concrete for bridges, US Navy Ships, and other concretes throughout World War I and II, without much knowledge on the internal processes taking place. The role of IC was

not documented until 1957 by Paul Kleiger, and major research has been underway since the mid-1990s by groups from Germany, the Netherlands, and Israel (Bentz et al. 2010).

CHAPTER 3

METHODS AND INSTRUMENTATION

The overall goals of the research performed on the large scale construction project was to determine the applicability of photocatalytic concrete pavements as well as the applicability of pervious concrete as highway shoulders, while the goals from the laboratory results were to determine the theoretical efficacy of photocatalytic pervious concrete. In order to accomplish these goals, the methods available were evaluated and a strategy to perform data collection and monitoring, operation and maintenance and to determine applicable results was organized. This chapter describes the methods selected and the instruments utilized to acquire data and determine results.

Water Quantity

Knowing that the rainwater runoff from the mainline will in fact be different than the water runoff from the shoulders, a method was implemented to segregate the sections by placing a tile drain at the edge of the mainline, allowing the runoff from the mainline to be captured immediately while a drain system was placed in the subbase to capture the runoff from the pervious concrete. A pipe from each section was then daylighted behind a sound wall, and connected to a V-notch weir box. The principle duty of the weir boxes is to

measure discharge, which is accomplished by measuring the height of water overflowing from the V-notch, after which the discharge can be back calculated. The weir box dimensions are provided in Figure 6.

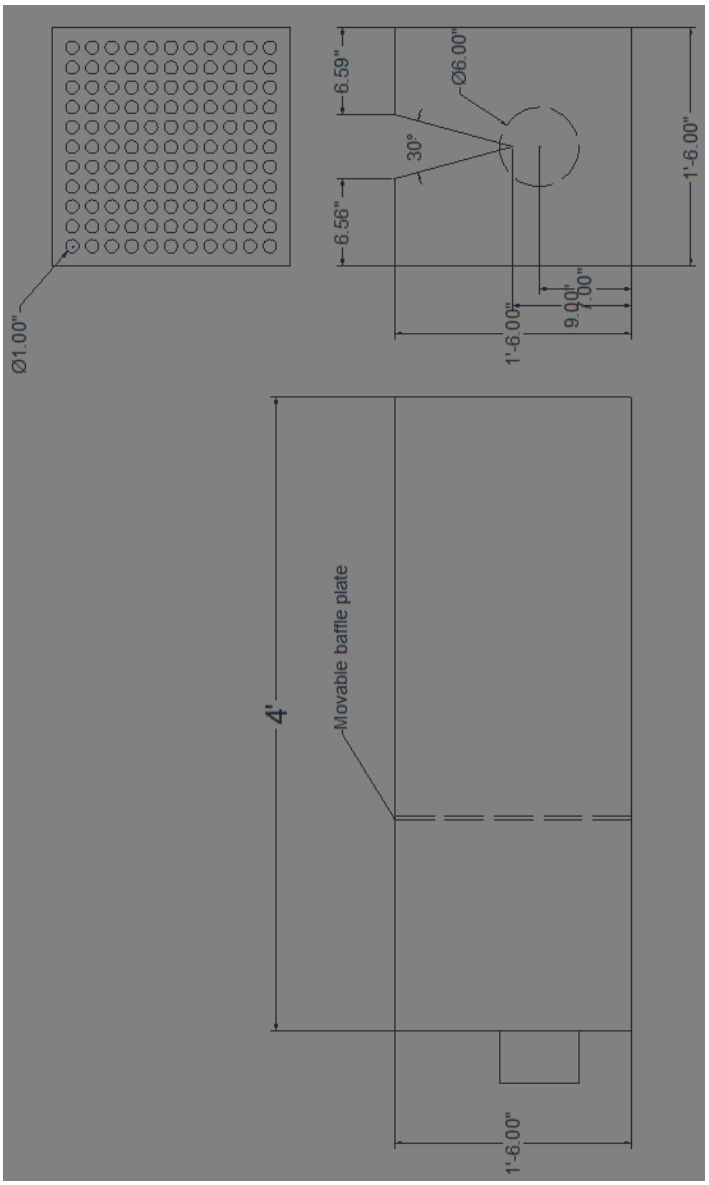

Figure 6. Weir box dimensions

The weir boxes were completed and then calibrated in a laboratory as shown in Figure 7. The results from this calibration are provided in Appendix A. The boxes were covered in the field, but opened during calibration for purpose of illustration.

Figure 7. Lab calibration of weir box

The depth of the water within the weirs was measured by Campbell Scientific CS450 pressure transducers, and the data was collected using a Campbell Scientific CR1000 data logger. In order to obtain representative samples of rain events, the data loggers were

programmed to take a reading every five-minutes; the data logger then stores this information until the data is downloaded on a computer.

The depth of the water in the subbase/pervious concrete was also determined in order to compute the water storage capacity of the system as well as the water retention time of the pavement. The pressure transducers used were the same as those used in the weir boxes, and were calibrated similarly and set to collect data every five minutes as well. The pressure transducer was placed in a standpipe, shown in Figure 8; the purpose of the standpipe was to house the instruments and to allow water percolation into the pipe to obtain accurate readings of water depth and retention time. ASTM test standard C1701 “Standard Test Method for Infiltration Rate of in Place Pervious Concrete” was used to determine the infiltration rate of the pervious concrete.

Figure 8. PVC perforated standpipe for instrument housing and water seepage

Laboratory pervious concrete samples were 16-inch by 16-inch by 3-inch, and the mix design is provided in Table 1. The samples were adjust slightly for better consistency, thus are slightly different than one another. Infiltration was determined using ASTM C1701, as shown in Figure 9. The void ratio of the specimens was determined using ASTM C1754 (2012). The samples were then placed in a flume that flows water on the surface of the concrete allowing the water to infiltrate the sample as shown in Figure 10 below. The amount of water entering the flume is measured using a Venturi tube, and the infiltration into the pervious concrete sample was measured using a V-notch weir as was the runoff from the surface of the sample. The flume was set to a 2% slope, which was the slope used on the highway, so as to provide comparable results to what would be observed in the field. One sample of both the conventional pervious concrete and the photocatalytic pervious concrete was used for this test.

Table 1: Lab sample mix designs

	PC (PCY)	TX Active (PCY)
Cement	506	506
Coarse	2033	2192
Fine	359	200
Fibers	1.5	1.5
Water	177	202
Super Absorbent Polymer (oz/cwt)	2	2
High Range Water Reducer (oz/cwt)	4	4
Stabilizer (oz/cwt)	4	4
Air Entraining Agent (oz/cwt)	1	1

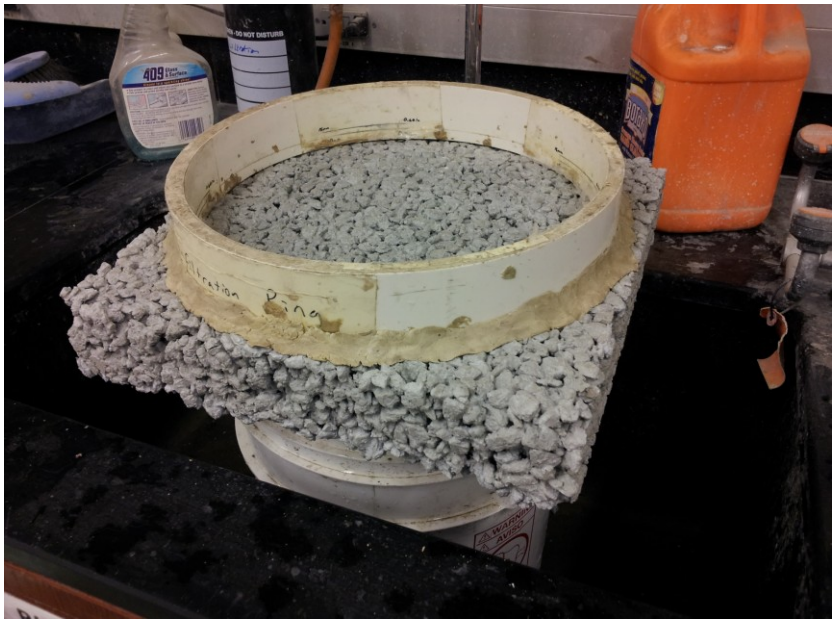

Figure 9. Infiltration ring to determine the rate of infiltration in pervious lab samples

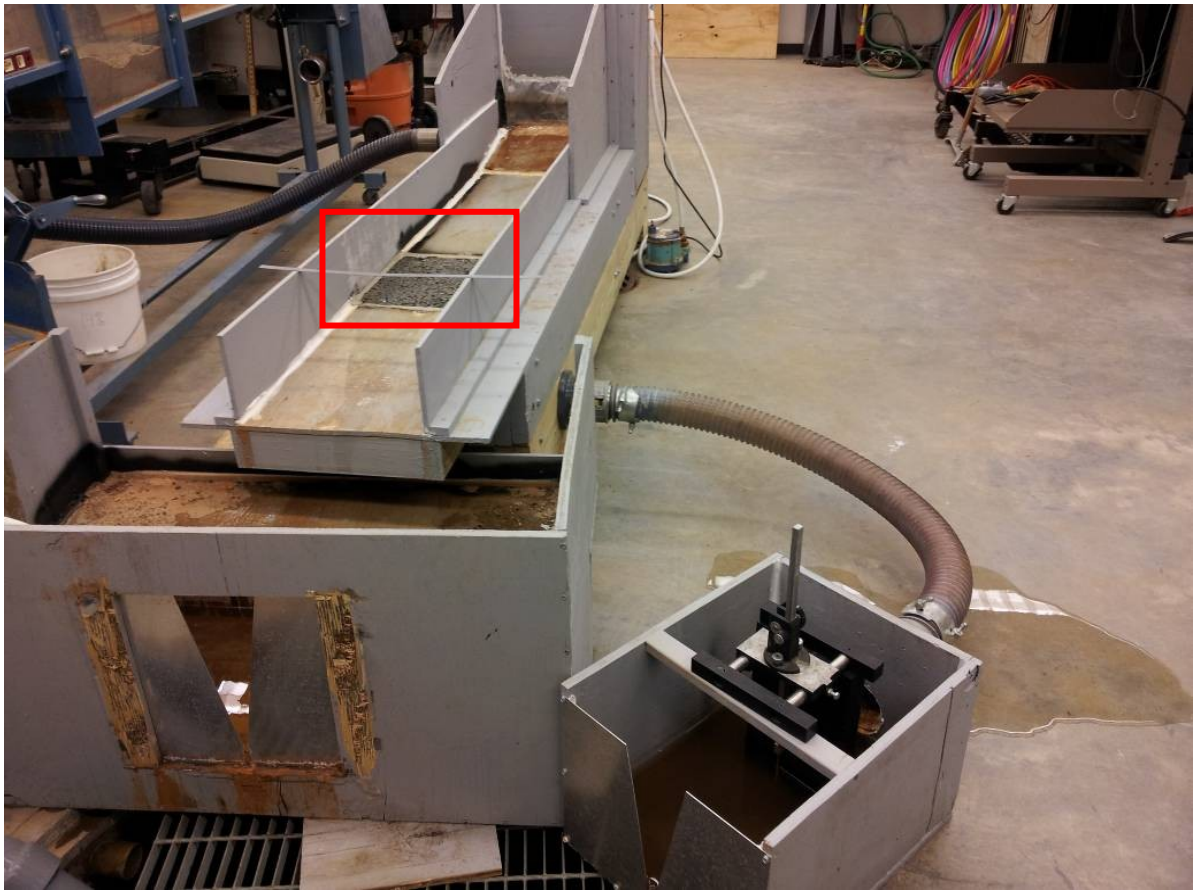

Figure 10. Flume used determine the infiltration rate of the samples (highlighted)

Water Quality

In the field, water samples were collected from the weir boxes using automated water samplers manufactured by Global Water Instrumentation. The water samplers connected to the weir box collecting runoff from the pervious concrete shoulders were models WS700 and used single two-gallon containers each. The samplers from the mainline were models WS750 and used two separate pumps and collected the water into two one-gallon containers each.

The reason for the differing samplers was to capture and evaluate the differing stages of runoff for the mainline separately and to closely monitor the effects of the photocatalytic concrete on rainwater runoff quality. The samplers collecting the runoff from the pervious concrete were set to approximately collect the first 30-minutes of a rain event, thus were set to collect 1000 mL every five-minutes. One pump of the samplers connected to the mainline was set to collect the first 30-minutes (600mL every five- minutes), while the second pump was set to collect the entire duration of the rain event (50mL every five-minutes).

The concrete lab samples were placed outside near some vehicular traffic in sunlight for a number of days. The samples were washed before and after placing outside to determine the difference of the water quality. The samples were washed with two liters of deionized water in a customized apparatus, as shown in Figure 11.

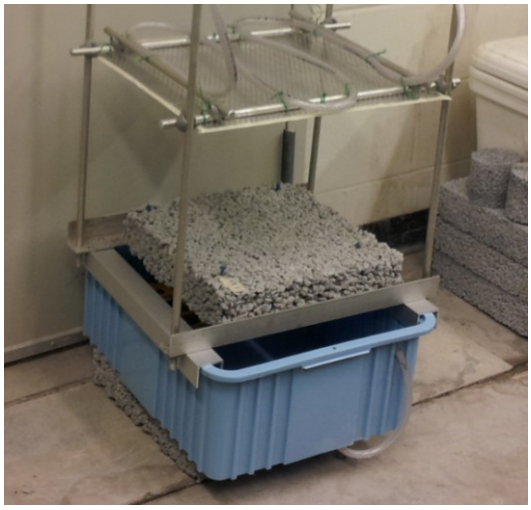

Figure 11. Water sprinkling apparatus used for mimicking rain events

After washing the samples after placing outside, the samples were then dried in an oven at 50° Celsius for 36 hours, and then were subjected to a stormwater sample. The storm sample was snowmelt from a local storm collected from a roadway gutter line in late February 2013, thus was expected to be worse than typical rain events due to the use of deicing chemicals and the higher concentrations of solids due to the accumulation of said solids in large snow piles in snow removal efforts. Therefore the snowmelt was diluted; roughly six liters of snow melt were mixed with 15 liters of deionized water for each concrete specimen. Afterwards, the concrete samples were washed in a mock rain event using the snowmelt samples, and the collected water was tested for the same parameters as was done prior to washing the concrete. The mock rain event was meant to mimic the water quality rain event, which in the St. Louis area amounts to a 1.14 inch storm as set by the Metropolitan St. Louis Sewer District (2006). In such a storm, roughly 114 cubic feet of water would fall on the pervious shoulder's watershed, which equates to roughly 0.6 cubic feet of water per square foot of pavement. Thus the 1.36 square foot concrete samples were washed with 0.776 cubic feet of water, or 22 liters. The water was poured so as to place 23% of the sample for the first hour, 54% for the second hour, and 23% for the third hour. This was meant to accelerate but somewhat mimic a Type 2 rain event, which is what is observed by the St. Louis Metropolitan area (U.S. Department of Transportation 2001).

The analysis performed on all of the water samples included measuring total suspended solids (TSS) using glass filtration, determining the pH and turbidity of the samples using specific apparatuses, and determining the anions in the sample using ion

chromatography (IC) to determine the reactivity of the photocatalytic concrete. The anions that were detected include nitrite, nitrate, phosphate, fluoride, bromide, sulfate, and chloride. The IC system was manufactured by Dionex and the systems model number was ICS-90. The IC performs isocratic ion analysis using suppressed conductivity detection, and the system must be calibrated for each anion that is to be detected. The calibration for the anions was completed using a standard solution with at least three different concentrations. This was to ensure adequacy of the ion detection and provide an elevated confidence interval.

Temperature and Solar Radiation

To determine the effect of the pavement profiles on the highway, T-wire thermocouples were installed into the pavements at differing depths to determine the temperature differences of the pavement due to the interaction of the differing layers. The T-wire sensors were connected to the CR1000 data logger, and the data collection rate was set to five-minutes. The pavements albedo was measured using an albedometer, composed of two Campbell Scientific CMP3 pyranometers, in order to determine the ratio of solar radiation reflected from the pavement with respect to the global solar radiation at the construction of the pavement. One of the two pyranometers measured the reflection of the pavement, while the other one measured the ambient ultraviolet radiation, as shown in Figure 12. This test was in accordance with ASTM E1918 “Standard Test Method for Measuring Solar Reflectance of Horizontal and Low Sloped Surfaces in the Field” (2006).

Figure 12. Albedometer composed of two pyronometers measuring initial reflectance of the pervious concrete pavement.

The lab samples were placed outdoors for 6 days with a CMP3 pyranometer nearby to determine the solar intensity for the duration of the solar exposure of the samples, as shown in Figure 13. The samples were placed so as to absorb uninterrupted ultraviolet radiation, near a minor source of vehicle traffic to determine the air quality benefits of the photocatalytic sample.

Figure 13. Samples placed outdoors with pyronometer recording solar radiation

Color analysis was performed on a TX Active pervious concrete sample colored with rhodamine dye and cured with soy bean oil, similar to what was used in the field. The samples were placed outside for five days, and were photographed under the same condition after each day. The pictures were then analyzed using image analysis software.

Material Testing

The highway building material was tested for differing properties. The only testing performed on the two-lift pavement was determining the compressive strength of the concrete of each lift using the ASTM C39: "Standard Test Method for Compressive Strength of Cylindrical Concrete Specimens" (2006) The specimens were collected and cured in a curing tank according to ASTM C31 (2006). The characteristics of the subbase beneath the pervious concrete including gradation, specific gravity, absorption, and unit weight were determined using ASTM C136, ASTM C29, and ASTM C127, respectively (2006; 2009;

2012). The gradation requirement of the material was compared to the ASTM D1241 "Standard Specification for Materials for Soil-Aggregate Subbase, Base, and Surface Courses" (2007).

Weather Station

Weather data was collected for temperature, humidity, wind speed and direction, solar radiation, and rain intensity and duration. All of the equipment was manufactured by Campbell Scientific and was meant to work and be programmed with the CR1000 data logger to collect data every five-minutes. The temperature and humidity was determined using a CS215 temperature and humidity probe; wind speed and direction was determined using a RM Young 03002 wind sentry; solar radiation was determined using a CS300 pyronometer; and rain intensity and duration was determined using a TB4 tipping bucket rain gauge. Prior to installation, the equipment was verified to ensure proper operation. A figure of the lab verification is provided below in Figure 14.

Figure 14. Weather station calibration prior to field installation

CHAPTER 4

LABORATORY SIMULATION

The laboratory simulation of the highway project was meant to supplement the results of the highway application. An overview of the tests completed and the results determined is provided within this chapter.

Color analysis was performed on TX Active pervious concrete cured with the same curing compound used in the field and colored with a rhodamine dye. The results of this test are provided in Figures 15 and 16.

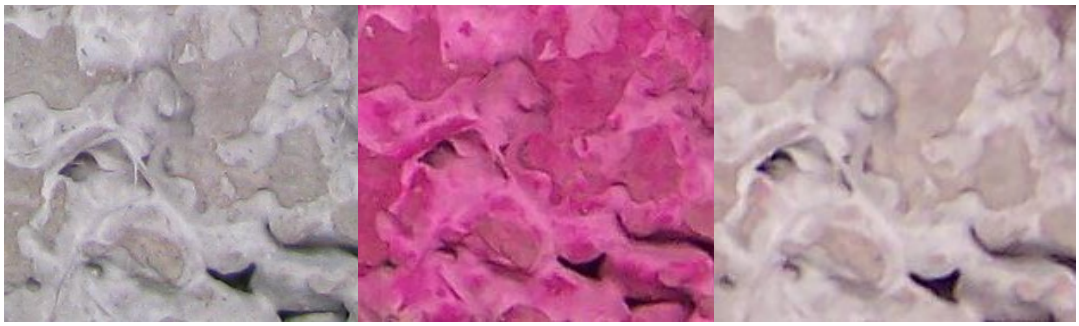

Figure 15. TX Active sample after placing (left), after painting with rhodamine dye (center), and after placing in sunlight and washing (right)

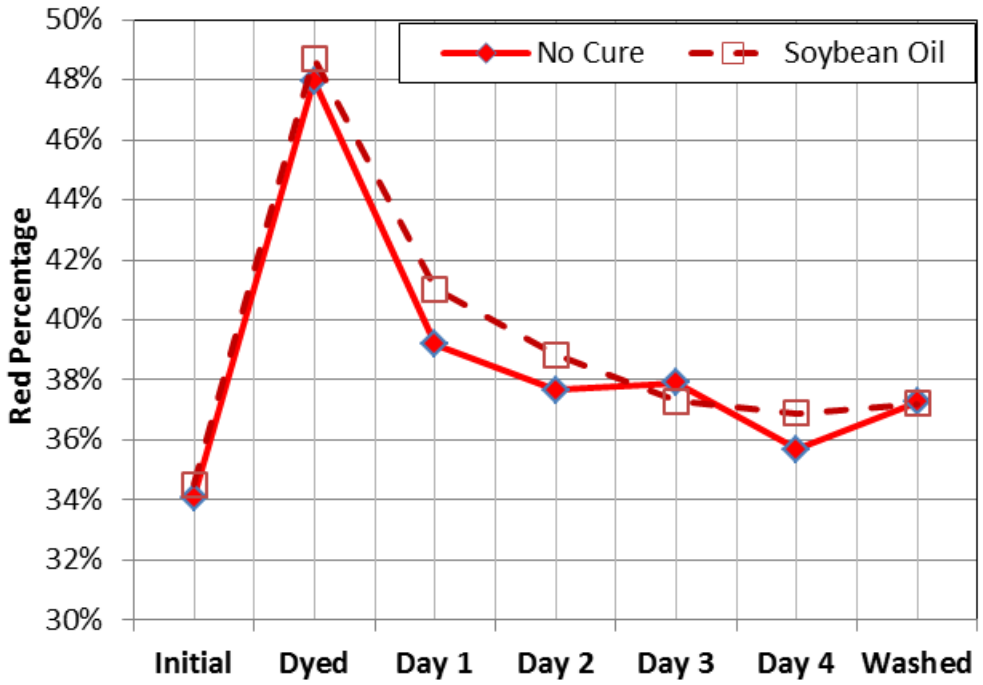

Figure 16. Color analysis of the rhodamine dye on TX Active pervious concrete

This test indicated that the rhodamine dye had increased the percentage of red on the surface of the sample after it was dyed, followed by the decrease in this value over time placed in sunlight. One day of placing in sunlight decreased the percentage of red associated with the dye by nearly 10%. Though the sample did not return to its original color, it did react with the sunlight to reduce the surface pollutants, in this case the dye.

A flowchart of the testing procedure associated with water quality is provided in Figure 17. Two pervious concrete samples were created using the selected field mixture in order to perform laboratory assessment on the pervious and photocatalytic pervious concrete. The laboratory simulation of the results included the analysis of the samples using a

hydraulic flume, water quality results of initial water effluent, solar irradiation of the samples, water quality data from the resultant water effluent after UV radiation, and then the simulation of a first flush event on the samples. These results are provided in order completed. The first test conducted on the samples was to determine the infiltration rate of the specimens for comparison purposes. These results are provided in Table 2, where the TX active pervious concrete sample is designated as TXPC, and the Portland cement pervious concrete is designated as PCPC. A summary of the void contents is also provided in Table 2. There were no replicates made for these two tests. The outcome that was determined was the photocatalytic concrete sample had nearly 6% more voids than the conventional pervious concrete. Along with the infiltration results, this data establishes that the samples were different than one another in terms of permeability.

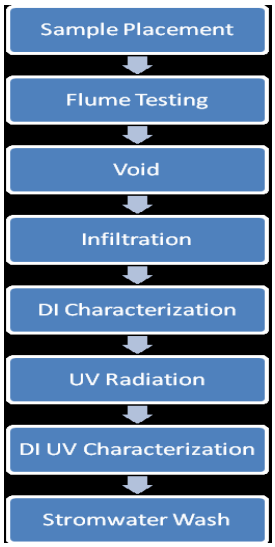

Figure 17. Flowchart of testing procedure

Table 2. Infiltration rate and void content of pervious concrete samples

	Infiltration	Voids (±2.2% Precision)
TXPC	1850 inches/hr	34%
PCPC	508 inches/hr	28%

The flume results are provided in Figure 18 for the PCPC and Figure 19 for the TXPC. The data associated with the flume is provided in Appendix B.

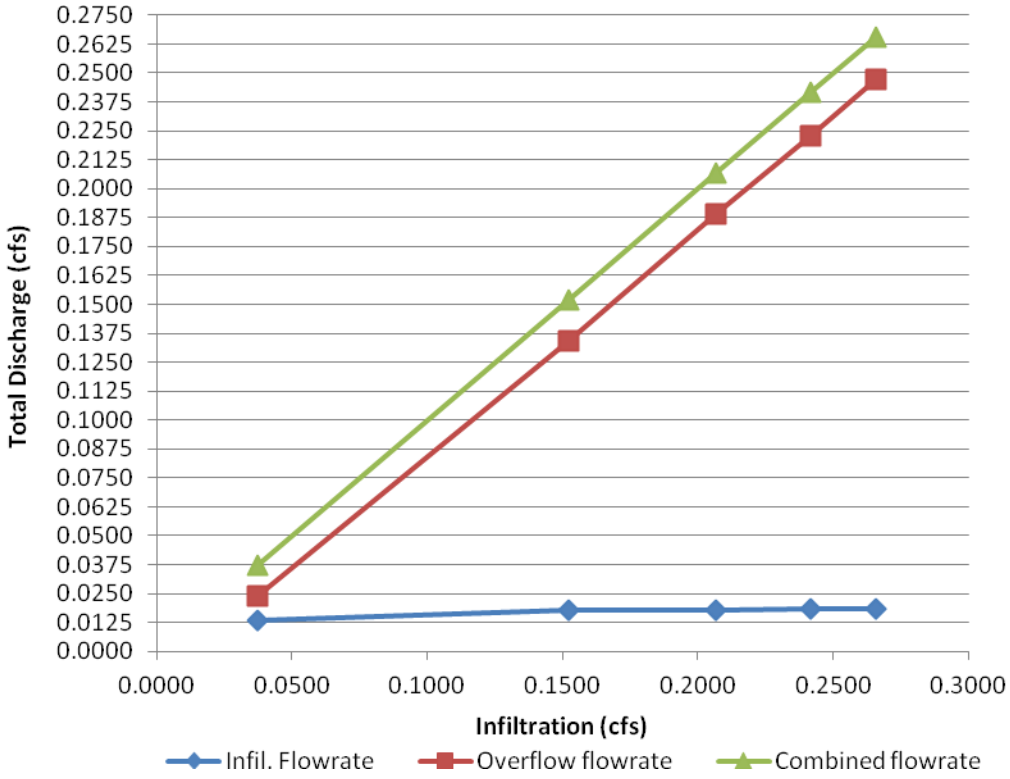

Figure 18. Infiltration rate of the Portland cement pervious concrete sample.

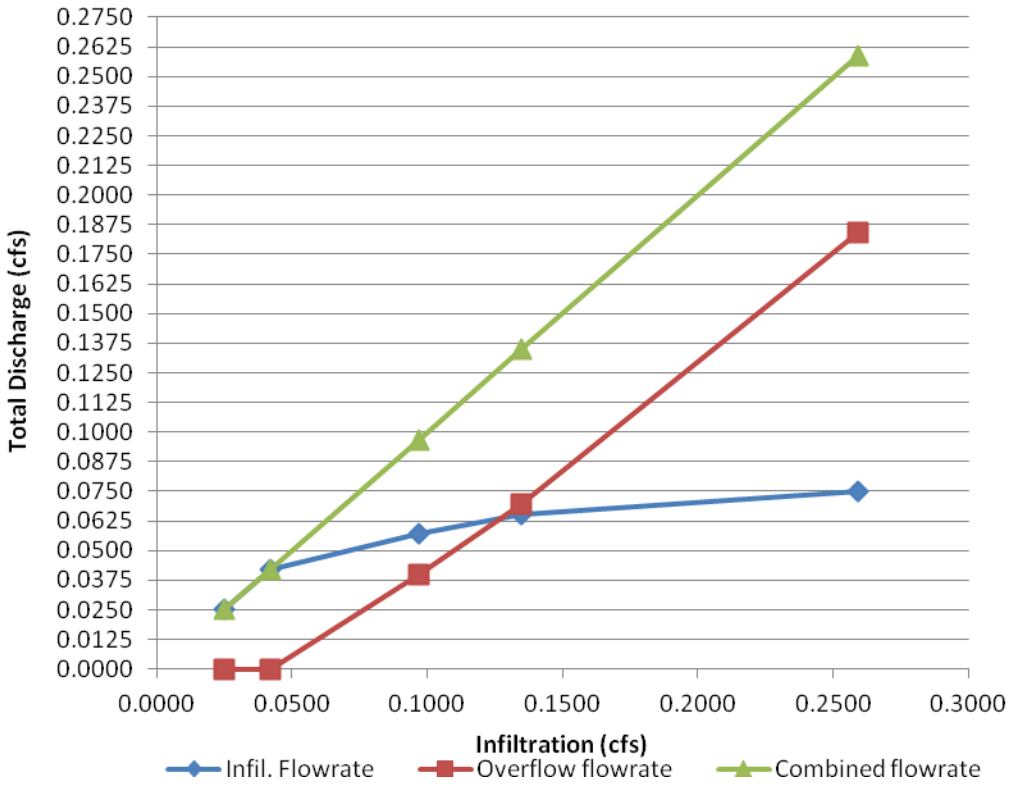

Figure 19. Infiltration rate of the TX Active pervious concrete sample

The infiltration rate diagrams show that the Portland cement pervious concrete sample had an infiltration rate that topped out at approximately 0.018 cubic feet while the rest of the water ran off the surface of the sample. The TX Active concrete sample diagram shows that the sample had allowed the infiltration of approximately 0.0400 cubic feet of water per second before any water ran off the sample. The infiltration rate then topped out at approximately 0.075 cubic feet of water per second.

Table 3 provides the water quality of the deionized water washing the samples prior to solar radiation and Table 4 provides the ions present in those water samples. Water quality

testing that was conducted included determining the total suspended solids (TSS), the turbidity, and the pH of the water. This wash was completed after the infiltration testing conducted with potable water. Each test was completed with three replicates of each sample. Statistical analysis of the ion concentrations is provided in Appendix C.

Table 3. Water quality results for the deionized water baseline

	TSS (mg/L)				
Sample	Average	Std Dev	COV	Turbidity (NTU)	pH
Ctrl DI Effluent	36.00	0.00	0.00%	2.40	8.54
TX DI Effluent	77.33	9.82	12.70%	14.50	8.72

Table 4. Ion concentrations in baseline water samples

	Ion Quantities (ppm)						
Sample	Fluoride	Chloride	Nitrite	Bromide	Nitrate	Phosphate	Sulfate
DI Water	--	0.039	--	--	--	--	--
Ctrl DI Effluent	0.107	1.053	0.067	--	0.156	1.419	11.035
TX DI Effluent	0.098	1.090	0.040	--	0.211	0.901	10.355

Table 3 shows that there were higher concentrations of solids on the concrete samples than expected, as these samples should have been cleaned properly. From Table 4, it was determined that the nitrates were not significantly higher in the TXPC than in the PCPC samples. The sulfate levels were high, possibly due to sulfate leaching from the hydration

process of the concrete, and there was a significant difference between them. The nitrites were also significantly different.

Figure 20 below presents the solar radiation of the days that the samples were placed outside. The results show the maximum radiation in one day, the minimum radiation in one day, and the average radiation amongst the six days.

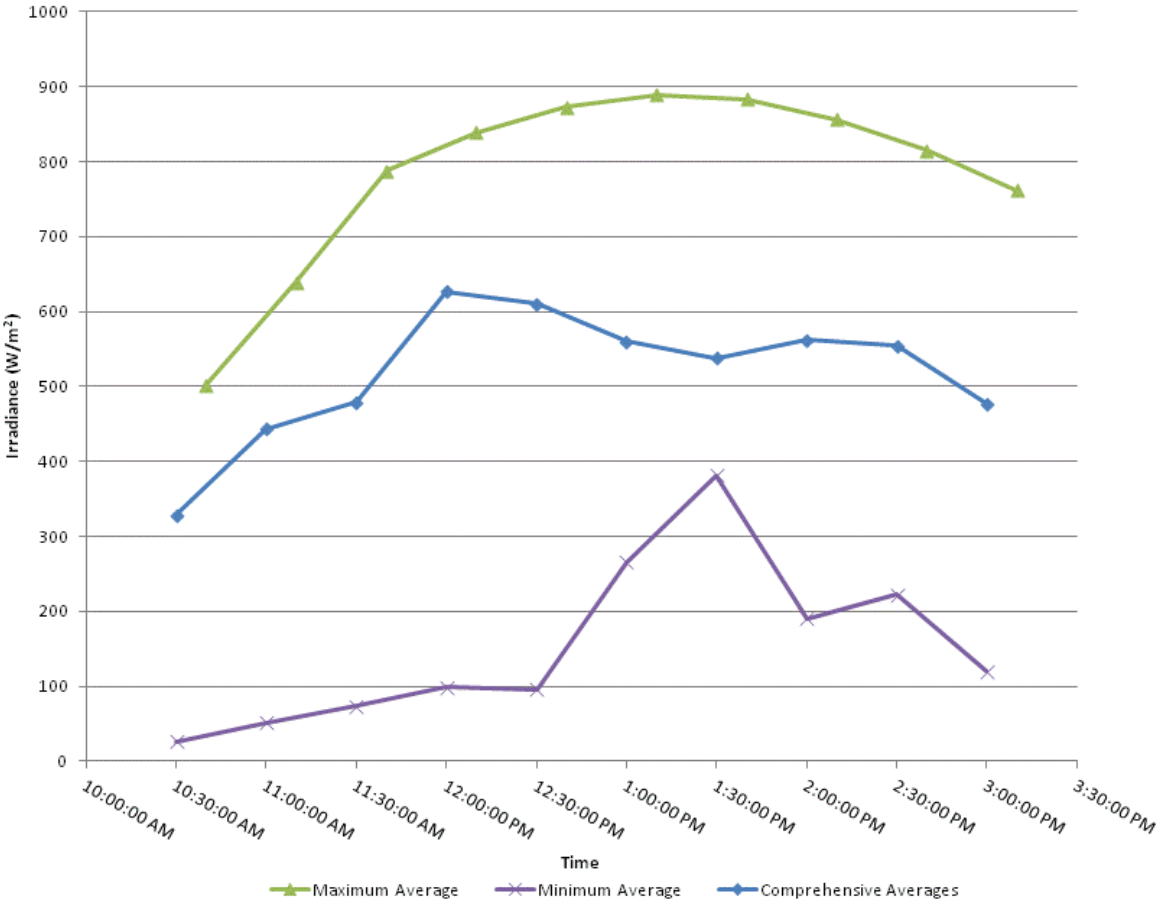

Figure 20. Solar radiation while the samples were placed outside

Table 5 quantifies the water quality of the deionized water wash after UV irradiation and Table 6 depicts the ions present in those water samples. Each test was completed with three replicates for each sample. Statistical analysis of the ion concentrations is provided in Appendix C.

Table 5. Water quality results for deionized water wash after UV

	TSS (mg/L)				
Sample	Average	Std Dev	COV	Turbidity (NTU)	pH
Ctrl UV Eff	25.33	0.67	2.63%	2.18	9.55
TX UV Eff	39.56	6.84	17.3%	4.90	8.95

Table 6. Ion concentrations in deionized water wash after UV

	Ion Quantities (ppm)						
Sample	Fluoride	Chloride	Nitrite	Bromide	Nitrate	Phosphate	Sulfate
Ctrl UV Eff	0.191	1.686	0.058	--	0.500	0.887	14.282
TX UV Eff	0.100	1.422	0.069	--	0.514	1.056	13.501

Table 6 indicates that the chloride and nitrate levels increased for both samples. The statistical analysis determined that the nitrate and phosphate levels were not significantly different for the control or the test sample, and all other ions were significantly different. The nitrite level of the TXPC was significantly higher than that of the PCPC, indicating the reactivity of the TX Active cement.

After the samples were irridated with solar light, and after they were washed with deionized water and dried, the collected stormwater sample was poured over the pervious concrete specimens to mimic a rain event. The specimens were not irradiated after washing with deionized water. Table 7 quantifies the water quality of the stormwater baseline and effluents of the samples and Table 8 depicts the ions present in those water samples. Each test was completed with three replicates for each sample.

Table 7. Water quality results for stormwater samples

	TSS (mg/L)				
Sample	Average	Std Dev	COV	Turbidity (NTU)	pH
Baseline Storm	190.67	13.32	6.98%	32.40	7.85
Ctrl Storm Effluent	185.33	5.03	2.72%	50.20	7.89
TX Storm Effluent	176.89	8.04	4.54%	34.60	7.65

Table 8. Ion concentrations in stormwater samples

	Ion Quantities (ppm)						
Sample	Fluoride	Chloride	Nitrite	Bromide	Nitrate	Phosphate	Sulfate
Baseline Storm	0.015	204.677	0.039	--	0.413	--	19.155
Ctrl Storm	0.040	226.469	0.138	--	0.670	--	29.361
TX Storm	0.041	199.288	0.136	--	0.593	0.706	28.342

Analysis of Laboratory Results

The samples that were being studied were determined to be different than one another with respect to the infiltration rates; however, the highway material was not available to create more samples, thus the samples would preliminary suffice for determination of water quality improvements. Upon placement in the flume, the TXPC sample was capable of entirely infiltrating more than 0.04 cubic feet per second. The voids, as previously mentioned, are approximately 6% greater in the TXPC than in the PCPC.

The water quality results of the deionized water effluent indicate that the samples needed better cleaning after running in the flume and measuring voids, as there was a higher concentration of solids than expected due to the solids within the water from both of those sources. After placing the samples in sunlight for six days, the deionized water wash had reduced solids. There were slightly higher concentrations of all ions in the TXPC after the irradiation, while the PCPC ion concentrations were varied. The nitrate ion concentrations, being the most significant indicator of photocatalysis reactivity as indicated by the literature survey, is somewhat unexpected, as there was an increase in concentrations in both the TXPC and PCPC, and the levels not being significantly different as proven by the analysis of variance. However, the TXPC did have a significant increase in nitrites. Though the samples seemed to have increased the same amount of nitrates, the increase in nitrites would suggest that TXPC reacted with NO gas to form nitrite, but did not complete the reaction due to the lack of hydroxide ions. This could possibly be due to inadequate humidity on the days that the samples were placed outside, or due to the lack of time the samples were placed outside.

Furthermore, another surprising find was similar sulfate increases. This may be associated with the low traffic volume of the road and the lack of smog present at the location where the test was conducted. The sulfate that was present may have been due to sulfate leaching from the gypsum within the cement. The TXCP did not seem to have any major effect on the water quality on stormwater that was used to wash the sample without UV irradiation.

CHAPTER 5

CONSTRUCTION

The construction process for the part of the highway that would be researched began in the Fall of 2011. The completion and grand opening of the highway to the public was in the Summer of 2012. The grand opening signified the end of all heavy construction; however, as of the grand opening, signage, retaining walls, sidewalks, and landscaping were still being completed as late as Spring 2013, according to the Missouri Department of Transportation's website (2012).

Photocatalytic Pavement

In order to pave the mainline highway with photocatalytic concrete, it was more economical to pave in two separate lifts, the bottom being a coarse, inexpensive lift, while the top lift being two-inches blended with photocatalytically active cement. Since this method is not common in the United States, the contractor had performed a test run of two-lift paving to ensure that the laborers understood the dynamics of the paving technique. Due to scheduling conflicts, the author was not available to attend the test run. The highway was paved on the 24th of October, 2011. The construction process began by placing the bottom lift with a typical slipform paving train. The concrete for the bottom lift was hauled on site, and

then placed on the base by means of a belt placer as shown in Figure 21, where it then passed a slipform paver, Figure 22. The bottom lift paving train was controlled and aligned using string line wire controls.

Figure 21. Concrete hauled in and placed with a belt placer

Figure 22. Slipformed bottom lift

The photocatalytically active top lift was placed using an asphalt materials placer as shown in Figure 23. The material was placed directly on top of the still fresh bottom lift where a second slipform paver processed the top concrete as shown in Figures 24 and 25. The top lift paver was controlled using a stringless guided system; the robotic total stations are shown in Figure 26. To minimize confusion of materials since both paving trains were operating simultaneously; trucks were unloaded on differing sides of the highway. The final stage of the paving train after mechanical and manual screeding of the top lift was the application of a curing compound with a cure cart.

Figure 23. Top lift placed in an asphalt placer and spread using a conveyor system

Figure 24. Top lift to be processed by slipform paver

Figure 25. Top lift after paver operation

Figure 26. Robotic total stations controlling stringless paver

Instrument Placement

After the initial two lift paving construction and other construction efforts such as grading the base, placing conventional shoulders, paving the northbound lanes, and placing Jersey barriers between the lanes were completed, the next phase of the UMKC research team was to begin placing instruments for data collection. This included placing instruments in the mainline and in the base beneath the pervious concrete. The instruments placed in the mainline were T-wire thermocouple wires, Figure 27. The instruments placed in the base include a perforated polyvinyl chloride (PVC) standpipe previously shown in Figure 8, and Figure 28 shows the field placement of the pipe. The standpipe housed a pressure transducer and T-wire thermocouples as shown in Figure 29.

Figure 27. T-wire thermocouples placed in the mainline pavement

Figure 28. Standpipes final placement

Figure 29. Standpipe in place and housing instruments

Shoulder Paving

After placing the instruments, and completing the drainage systems and placing the formwork for the shoulders as shown in Figure 30, the following step in the procedure was the paving of the pervious shoulders.

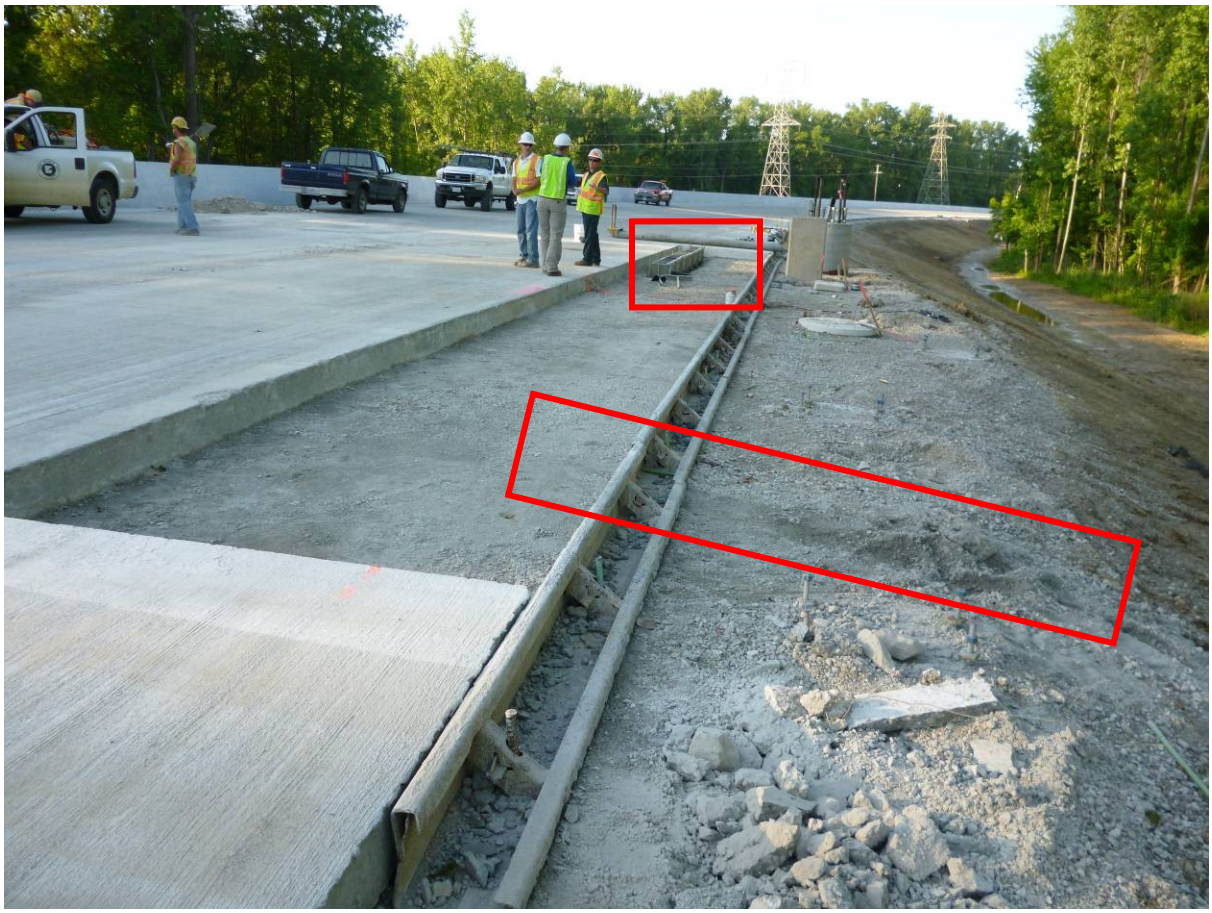

Figure 30. Completed formwork and the (highlighted) drainage systems.

In order for the final placement of the pervious concrete shoulders to take place, a trial placement was needed, as shown in Figure 31.

Figure 31. Final pervious concrete mix during test trial

The pervious concrete shoulders were paved on the 3rd of May, 2012. The pervious concrete was hauled on site using agitator trucks, at approximately 10 cubic yards per load. The conventional pervious concrete was the first to be placed, followed by the photocatalytic pervious concrete. To protect the equipment and wires, concrete was placed so as to cover the delicate items and to fill in gaps and holes prior to placing as shown in Figure 32. The material was spread using the agitator truck chute and hand tools, Figure 33, and was finished using a roller screed, Figure 34. Finishing around the tile drain and other difficult to reach areas was completed by hand as shown in Figure 35. After paving over the standpipe, the concrete was removed from the surface exposing the pipe as shown in Figure 36. After finishing, the shoulders were sprayed with a curing compound using a small pump sprayer as depicted in Figure 37.

Figure 32. Protecting wires and filling in low spots with material

Figure 33. Placing concrete using truck chute and hand tools

Figure 34. Roller screed finishing

Figure 35. Hand finishing around tile drain

Figure 36. Uncovering standpipe

Figure 37. Hand pressurized cure spray

Weir Box Placement

The weir boxes were connected to the pipes daylighted from the pervious concrete sections, and were installed on wooden foundations to protect and level the boxes as shown in Figure 38. Steel reinforcing bars (rebar) were placed in front of the wooden foundations to prevent sliding, highlighted in Figure 38, and steel shelf brackets were attached onto the boxes and placed in the ground, as shown in Figure 39. The rebar pieces used were 18-inches long and the steel brackets were approximately 3-feet long. The PVC weir boxes originally were covered with PVC lids; however, due to climatic conditions including excessive heat and sunlight, the PVC lids were replaced with wooden lids at the presence of warping, as represented in Figures 40. The lids, along with the wooden foundations, also served the purpose of supporting the box from bulging when filled with water.

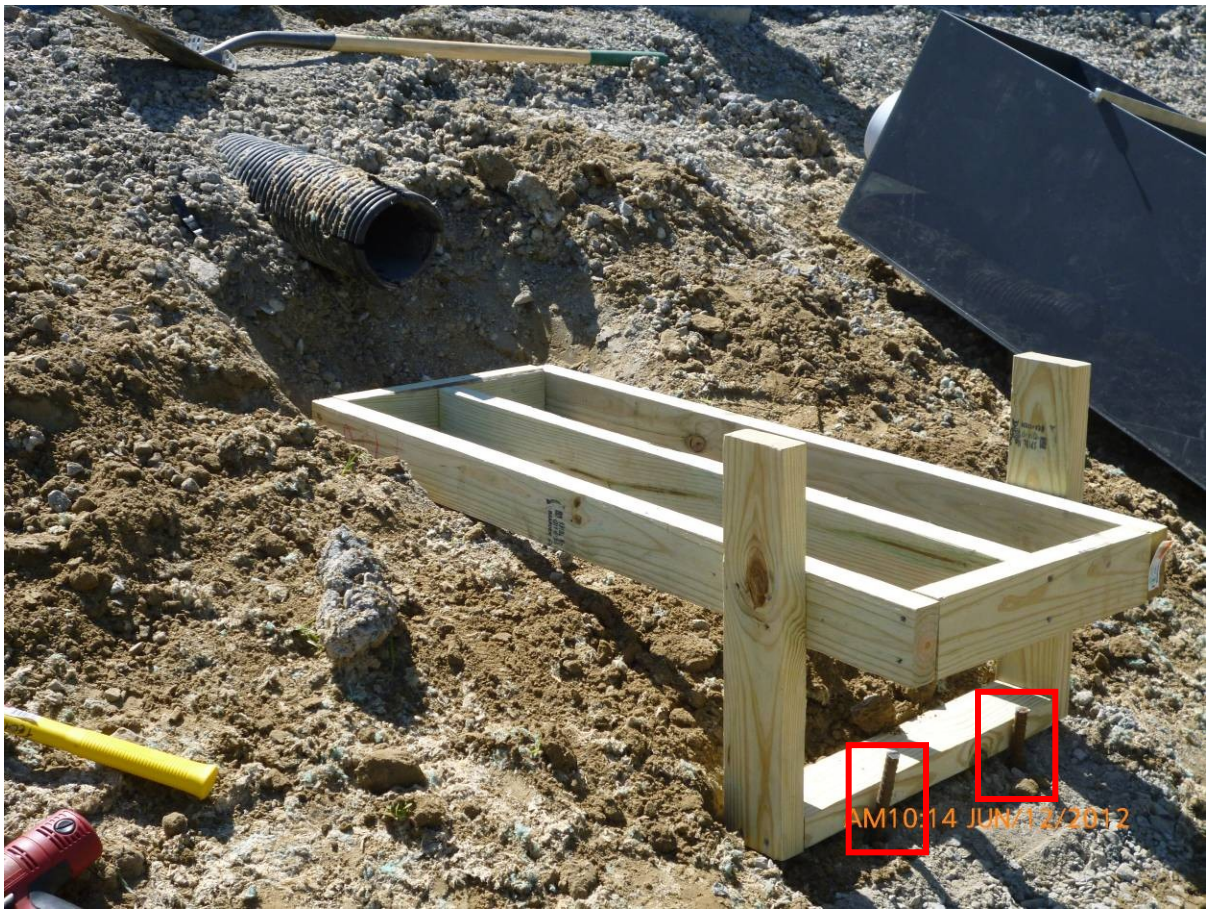

Figure 38. Wooden weir box support and reinforcing steel

Figure 39. Steel shelf brackets attached to the weir boxes to prevent slippage.

Figure 40. Wooden lid protecting the weir box from the elements

In order to further protect the weir boxes and the drainage ditches slope, riprap was placed beneath the boxes and at the base of the water discharge. This was repeated multiple times as the water flanked the slope differently each time that riprap was applied. Figure 41 and 42 below represent the finalized slope stabilization executed for one of the more aggressively eroded weir box locations.

Figure 41. Rearview of aggressive erosion due to water discharge from weir box

Figure 42. Riprap placement to protect drainage ditch slope from erosion

Equipment Vaults

All of the equipment was housed in one of two 4-foot by 4-foot by 4-foot concrete vaults located behind the sound wall that were placed after the pervious shoulder construction. One vault was located behind the photocatalytic concrete test section, and one was located behind the control section. These vaults were covered with a 2-foot heavy duty steel lid, and were to be connected to electricity from a nearby power source that also powered highway signage. The weather station was mounted to the vault behind the sound wall of the test section, and was elevated according to the installation requirements, as shown in Figure 43. The only exception to this was the wind sentry, which was initially attached to the vault, but then moved and placed directly to the sound wall, depicted in Figure 44. The

reason for the move was the fact that the sound wall was not constructed as of the initial instrument placement.

Figure 43. Weather station mounted directly to the vault, prior to moving the wind sentry

Figure 44. Wind sentry moved directly to the sound wall

The water sampler hose was trenched from the weir boxes to the appropriate vaults, as were all of the T-wire thermocouples, pressure transducer wires, and moisture sensor wires for the water samplers. The hoses and wires from the weir boxes are shown in Figure

45. All of the wires were inserted into the vaults from slots installed into the concrete prior to installation, as shown in Figure 46. Also depicted in the figure is the fact that the slots were sealed using spray foam insulation to prevent moisture intrusion.

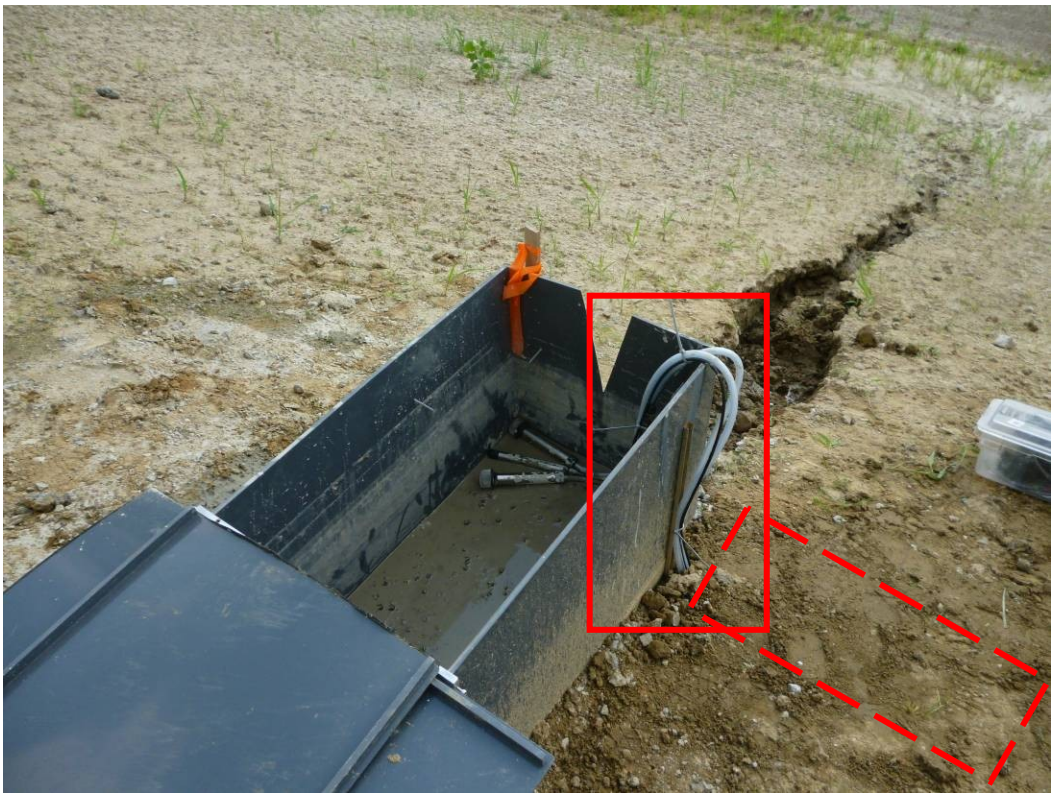

Figure 45. Wires and hoses buried and trenched to the concrete vault

Figure 46. Slot for wire and hose insertion within the concrete vault

Highway Completion and Ribbon Cutting

After placing the pervious concrete shoulders, the highway construction was completed with the addition of sound walls, Jersey barriers (and other safety provisions), highway markings, signage, and landscaping. The highway was opened to the public with an organized 10-kilometer "Run to Get it Done", followed by a reception where politicians and public figures discussed the improvements and undertakings, then a ceremonial ribbon cutting on July 14th, 2012. Pictures of the reception and grand opening are provided in Figure 47 and 48. Even after the grand opening, minor work was still being completed by the contractor, however, impact on drivers was supposed to be minimal.

Figure 47. Public gathering for reception and organized walk

Figure 48. Ceremonial ribbon cutting and grand opening of MO 141highway

CHAPTER 6

FIELD RESULTS

This section is meant to provide the results for the material testing, on site data, and water quality results. Due to problems that were encountered onsite, the results were deficient with regards to the actual highway, as some information such as weather data and pavement profile were lost with the water damaged instruments. These issues will be discussed in the following chapter; however, the issues were significant enough to restrain the entire test sections data acquisition, which also included the weather station. Furthermore, the initial water quality results may be flawed as the water samplers had leaked causing battery fluid to possibly seep into the samples. The results are provided in chronological order of completion.

Two-Lift Concrete

The two lift concrete was tested for compressive strength, as provided in Table 9 and 10. Both lifts were tested separately with three samples for each break. The results also provide the standard deviation and the coefficient of variation to determine the variance of the results.

Table 9. Bottom lift concrete compressive strengths

Day Tested	Average (PSI)	Std Dev	COV
28day	7384	215	2.91%
90day	7783	506	6.51%

Table 10.Top lift concrete compressive strengths

Day Tested	Average (PSI)	Std Dev	COV
28day	5218	126	2.43%
90day	5980	197	3.30%

Subbase Characteristics

The characteristics of the limestone subbase beneath the pervious concrete were determined to verify the water storage and infiltration capabilities. The dry rodded unit weight, the bulk specific gravity, the specific gravity at saturated surface dry conditions, and the absorption of the subbase material are provided in Table 11 below. The gradation curve for this material is provided in Figure 49.

Table 11. Subbase characteristics

DRUW=	91.5 pcf
SG_{Bulk}=	2.38
$SG_{Bulk,SSD}$=	2.51
ABS=	5.22%

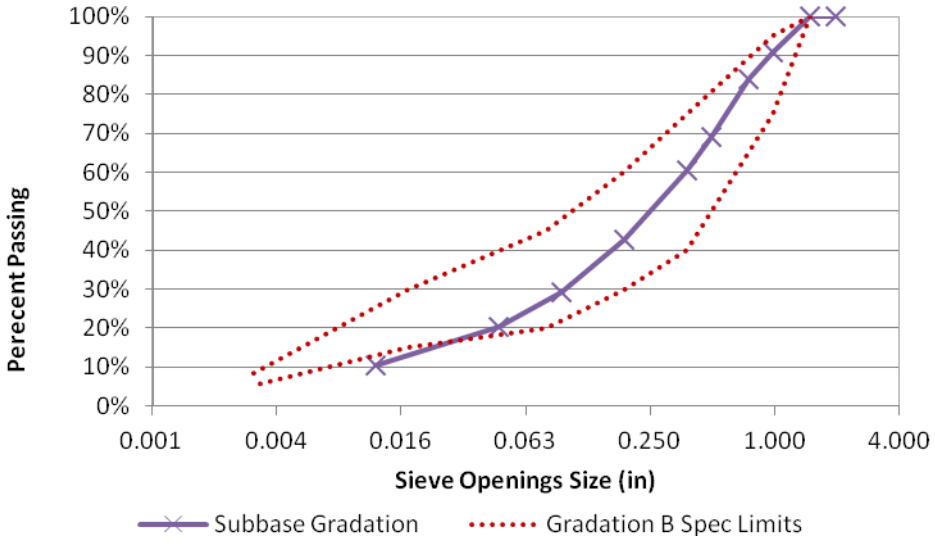

Figure 49. Subbase Gradation

The coefficient of uniformity for this curve is equal to 26.7, and the coefficient of curvature is equal to 1.7. This particular gradation curve most closely meets the "Gradation B" designation of the the ASTM D1241 (2007).

Albedo of New Pavement

The albedo of both the control and the test pavement sections was determined the day that the highway was opened to the public. The results are provided in Table 12.

Table 12. Albedometer readings

Location	Albedo
Control Mainline	0.31
TX Active Mainline	0.33
Control Pervious Shoulders	0.29
TX Active Pervious Shoulders	0.33

Weather Data

To make up for the lost weather data from the damaged data logger, weather information for the St. Louis area was obtained from the National Oceanic and Atmospheric Administration's Climatology and Weather Records (2013). Table 13 provides monthly averages for the Spring and Fall of 2012. Table 14 provides monthly rainfall totals for the same time period.

Table 13. Saint Louis, MO – Monthly and Seasonal Mean Temperature (F)

	SUMMER				FALL				YEAR	
YEAR	JUN	JUL	AUG	AVG	SEP	OCT	NOV	AVG	YEAR	AVG
2012	78.2	88.1	79.6	82.0	69.4	56.9	46	57.4	2012	61.2
AVG	75.3	79.6	77.8	77.5	70.2	58.7	45.4	58.1		56.3
MAX	83.1	88.1	84.9	82.7	77.4	66.9	54.4	63.5	1921	61.2
MIN	68.6	74.9	70.4	72.9	62.3	49.5	33.0	52.0	1875	52.8

Table 14. Monthly and Seasonal Rainfall (inches) Totals- Saint Louis, MO

	SUMMER				FALL				YEARLY	
YEAR	JUN	JUL	AUG	TOT	SEP	OCT	NOV	TOT	YEAR	TOT
2012	1.97	0.72	4.00	6.69	3.03	2.50	1.40	6.93	2012	32.30
Max	12.35	12.69	14.78	27.22	10.04	12.38	9.95	21.50	2008	57.96
Min	0.10	0.37	0.07	4.09	Trace	0.21	0.11	2.36	1953	20.69
Avg	4.15	3.49	2.98	10.64	3.15	2.78	2.92	8.78		37.65

The data logger from the control section was retrieved and the data was downloaded and processed for clarity. Figure 50 depicts the water depths throughout the time period of data collection of the mainline weir, the pervious shoulder weir, and the aggregate subbase. Figure 51 provides the temperature of the weir box and the water.

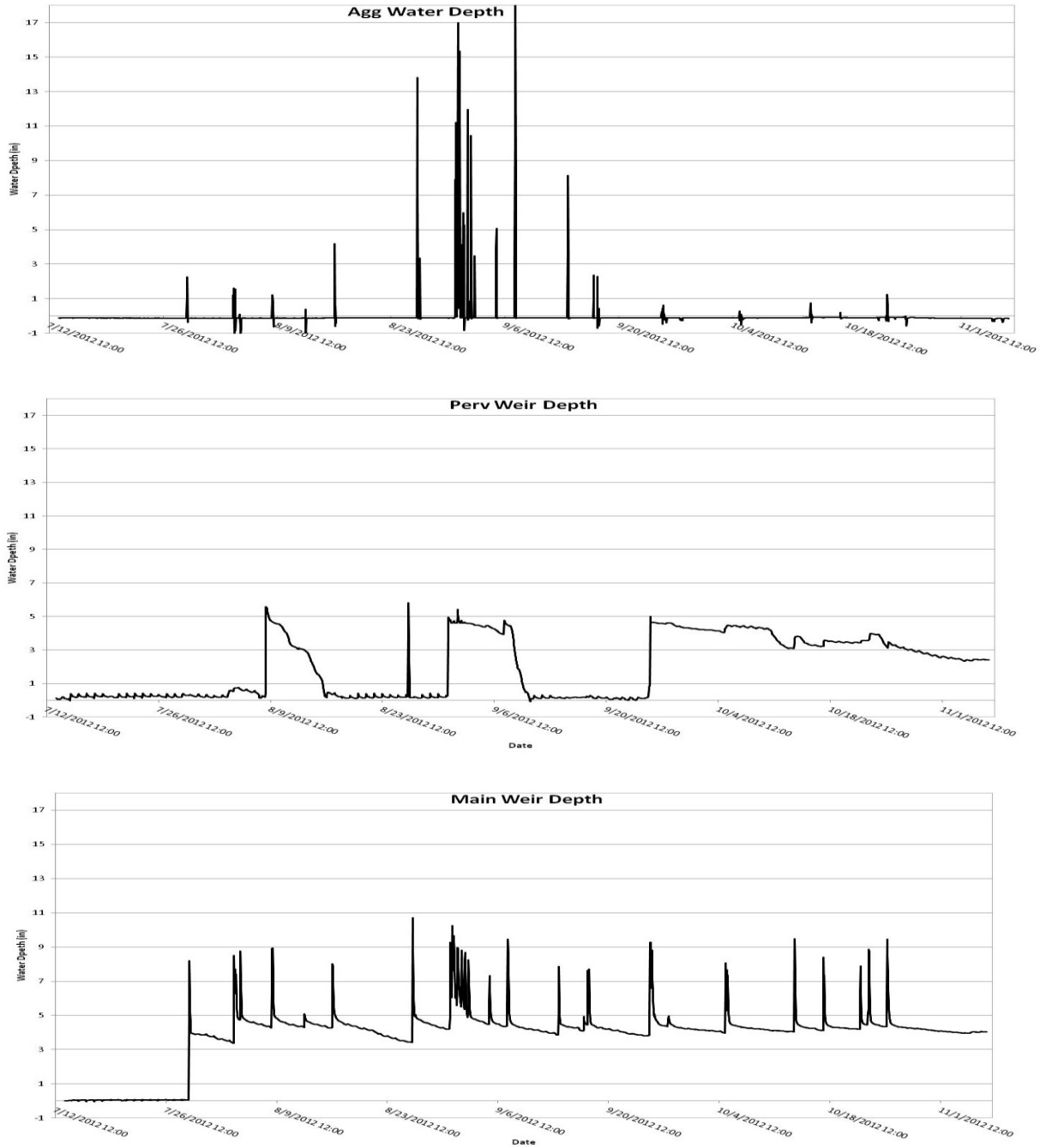

Figure 50. Depth of water within control section weirs from initial placement until the battery died, hourly averages

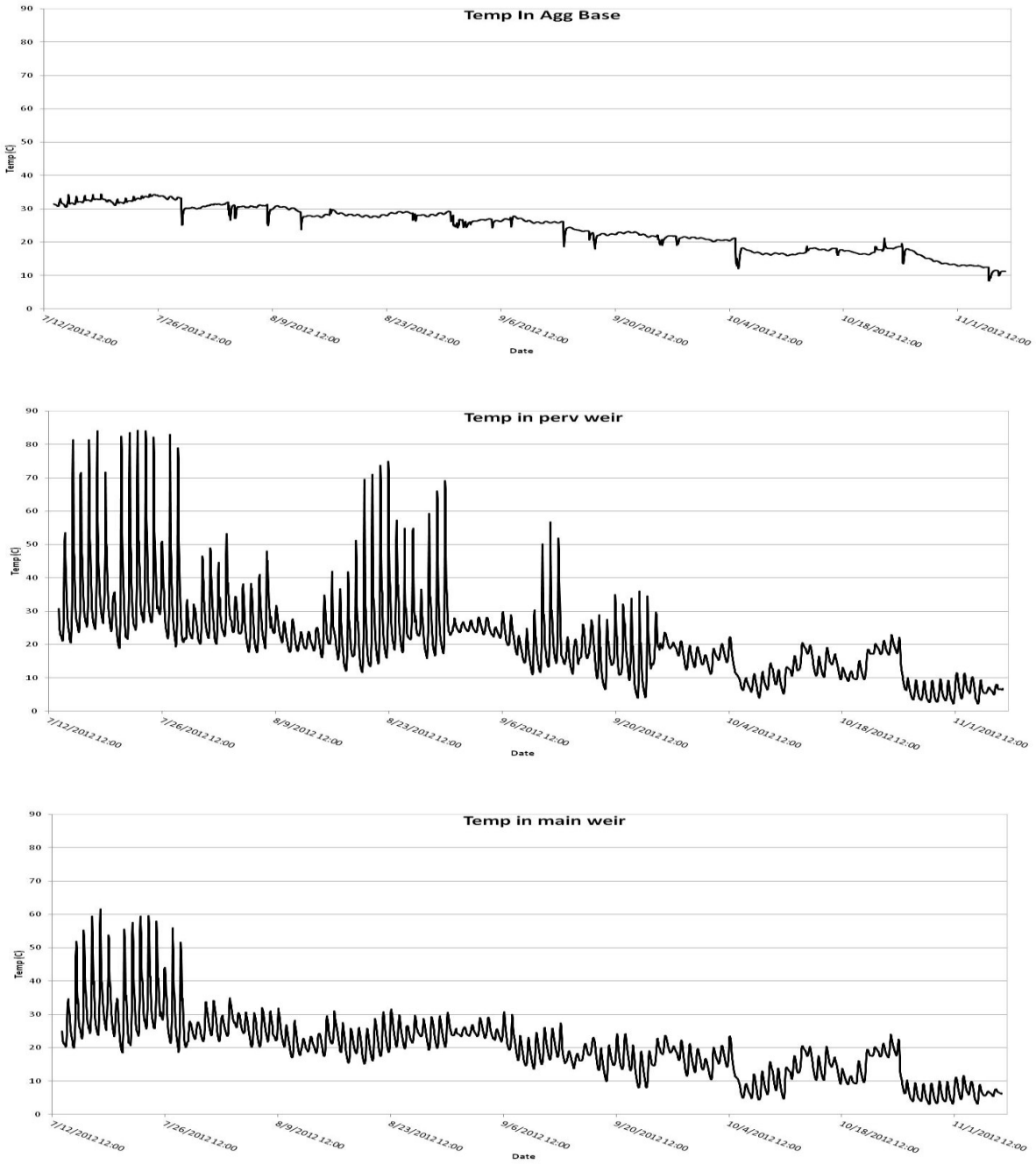

Figure 51. Temperature of water within control section weirs from initial placement until the battery died, hourly averages

The data depicted from the weir boxes indicate that the aggregate subbase allowed for quick drainage of the water which is shown by the rapid drop in water depth. The water in the pervious weir box decreased slowly over time. This indicates that the pervious shoulders continued to drain into the weir box, even after the rain event ended. In late September, the weir box drainage holes were clogged from debris. The first rain event had clogged the drainage holes of the mainline weir box, however, the water above the notch drained quickly. This shows that once the rain event ended, the weir box stopped collecting water, unlike the pervious weir.

The temperature profiles of the concrete are provided in Figure 52-55.

Figure 52. Pervious pavement profile temperatures

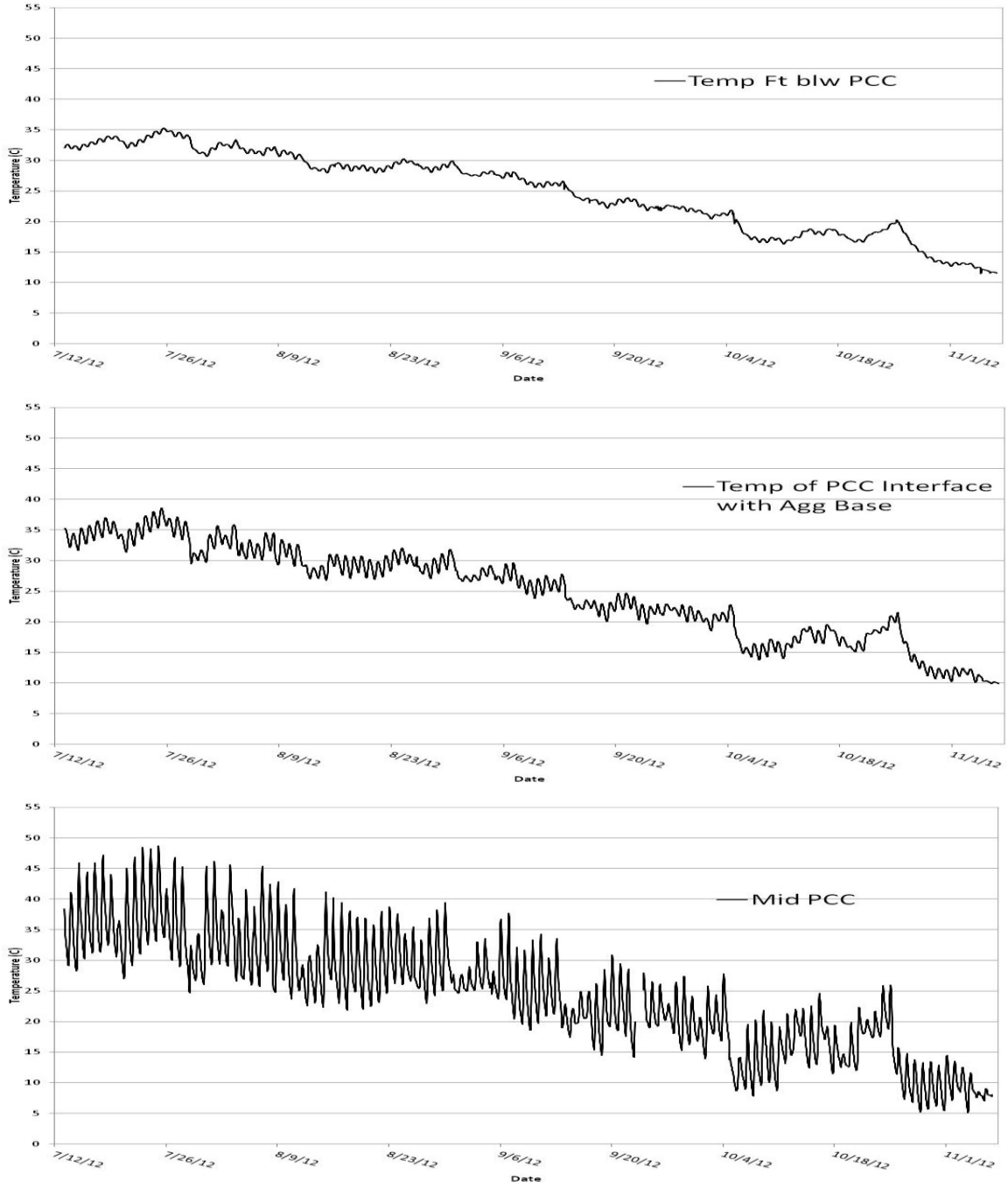

Figure 53. Mainline pavement profile temperatures

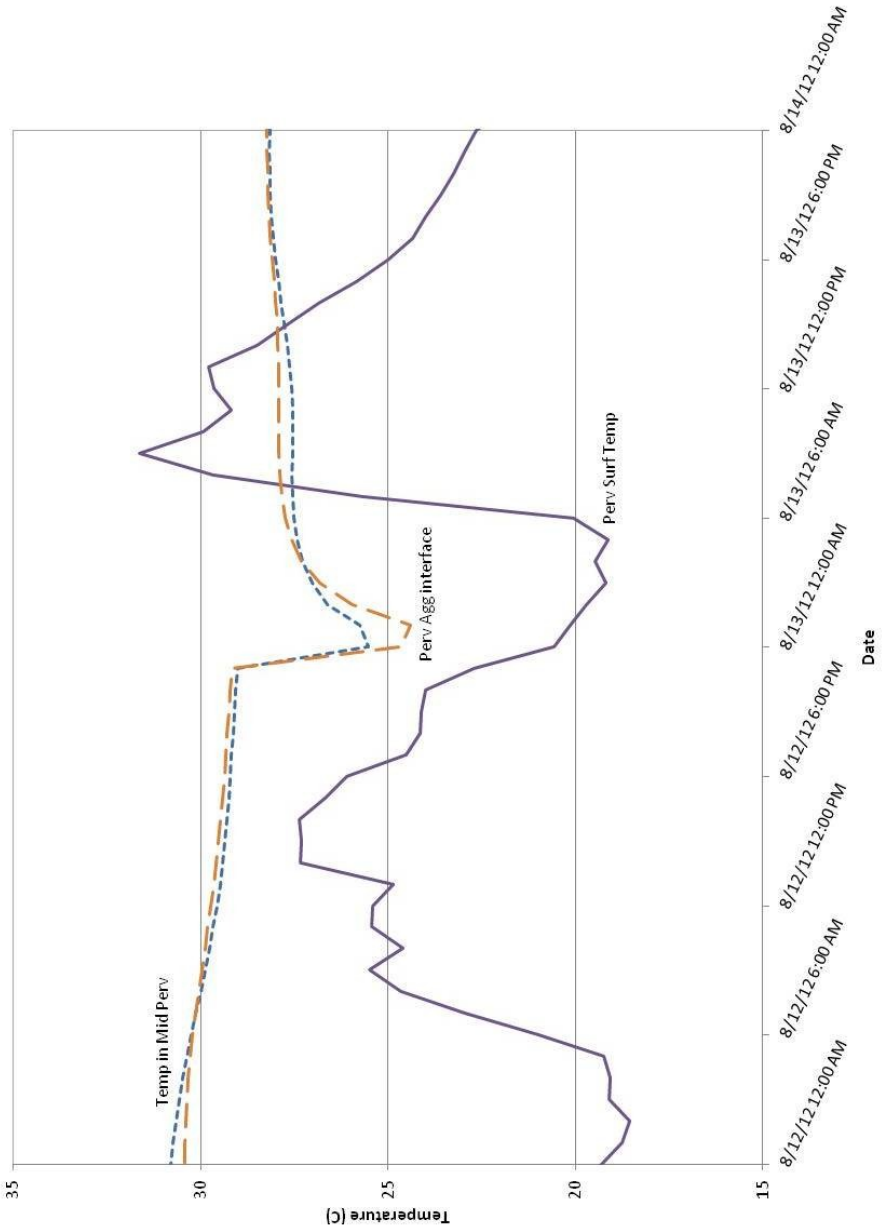

Figure 54. Pervious concrete temperature response to rain infiltration, approximately 24hours before and after rain event

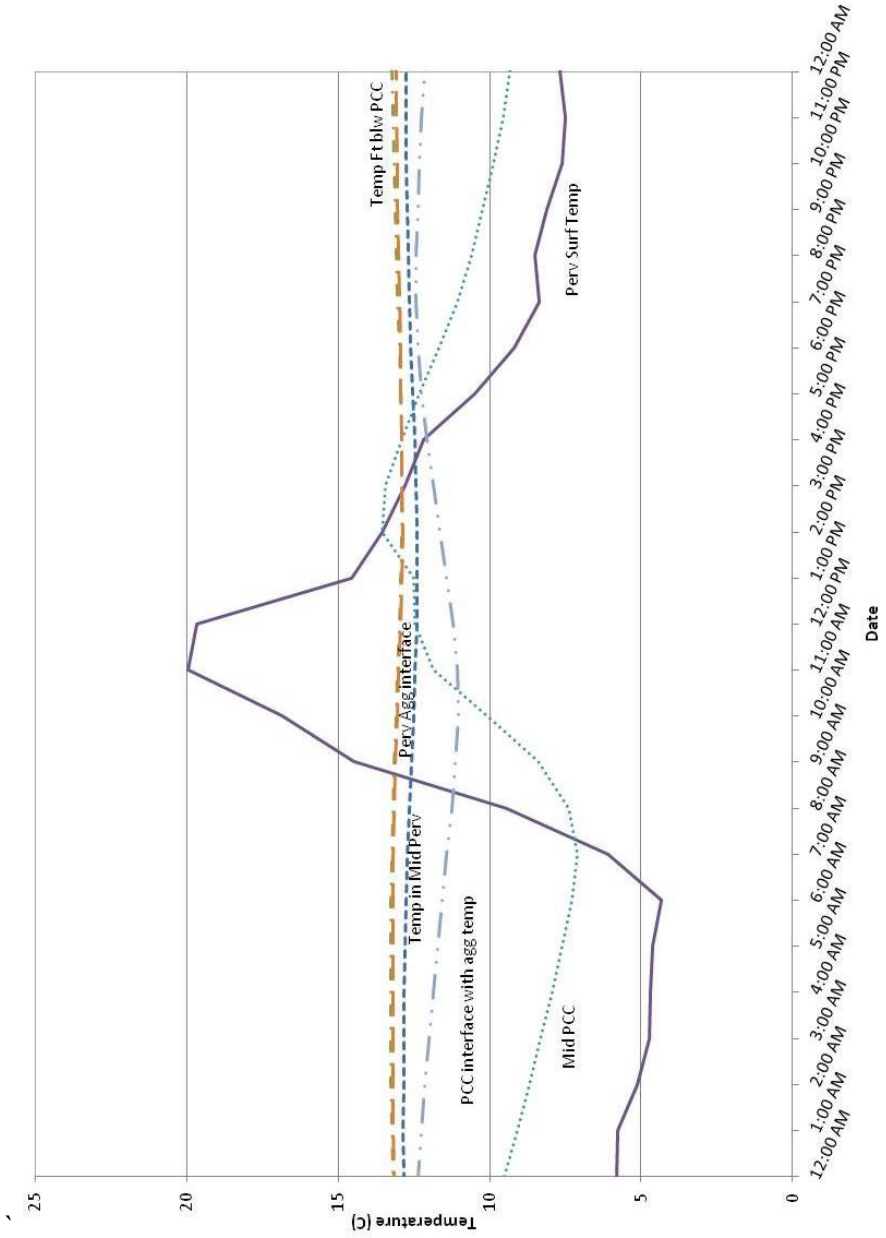

Figure 55. One day comparison of all temperature sensors, on 11/02/2013

The trend of the temperatures of the entire pavement decreased over time, which is expected as the weather becomes cooler with the change of seasons. The substrate fluctuated

slightly from day to day, but the surface temperatures fluctuated greatly. The dips in the temperature of the pervious substrate correspond to rain events. The mainline substrate temperatures also exhibit slight decreases in temperature; however, these dips are trivial in comparison.

Water Quality Results

Two sets of samples were collected from the automated water samplers on site, and the water was analyzed for TSS, pH, and turbidity as well as analyzed using the IC. The first sample was collected during the construction phase, when nonpotable water was used to wash the concrete. The second was from stormwater collected on July 29, 2012, which was the first presence of water in the weir. The automated samplers would have been filled completely at this point in time, thus all subsequent rain events would have not been collected. Table 15 provides the results of the TSS, acidity, and turbidity for the construction water collected from the mainline weirs, while Table 16 provides the results of the collected storm. The data for the construction water is taken from three replicates; however there is only one replicate for each sample from the first storm due to the lack of water. Figures 56-58 depict these results graphically and provide a comparison between the differing collection points. The water collected during construction is considered a grab sample, while the samples collected from the storm include the first 30 minutes of the storm for the mainline pavement of both the control and test sections (hereon referred to as first flush), the collection of 50 milliliters of water every 10 minutes (hereon referred to as the entire storm)

of the mainline pavement of both sections, and the first flush of the pervious concrete water samples.

Table 15. Mainline water quality, of construction water

	TSS (mg/L)				
Sample	Average	STD Dev	COV	Turbidity (NTU)	pH
PC Mainline Water	3377.67	358.85	10.62%	30.5	8.25
TX Mainline Water	374.00	12.86	3.44%	4.15	8.64

Table 16. Water quality of rainwater sample collected on 07/29/2012

Sample	TSS (mg/L)	Turbidity (NTU)	pH
PC First Flush	30.67	12.9	5.20
PC Entire Storm	33.50	11.5	6.14
PC Pervious	3.14	0.632	5.87
TX First Flush	38.00	4.470	5.89
TX Entire Storm	593.00	76.1	6.32
TX Pervious	1.60	0.765	6.01

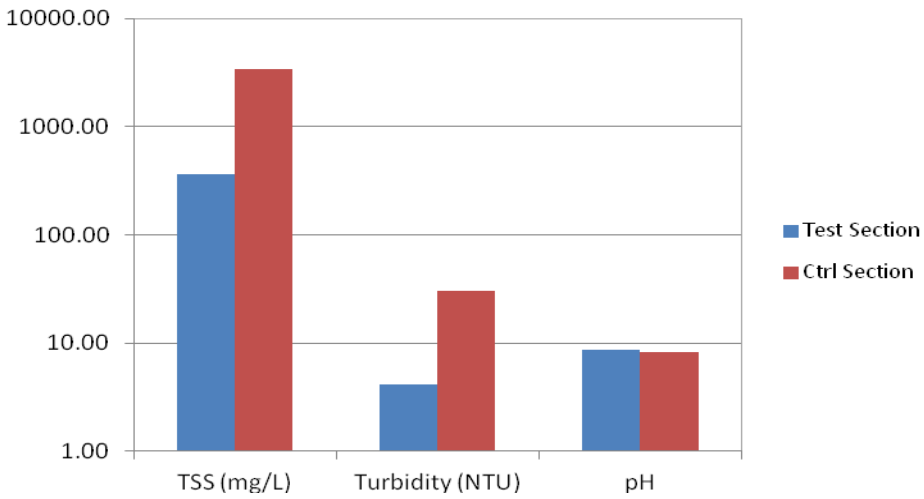

Figure 56. Construction water quality results

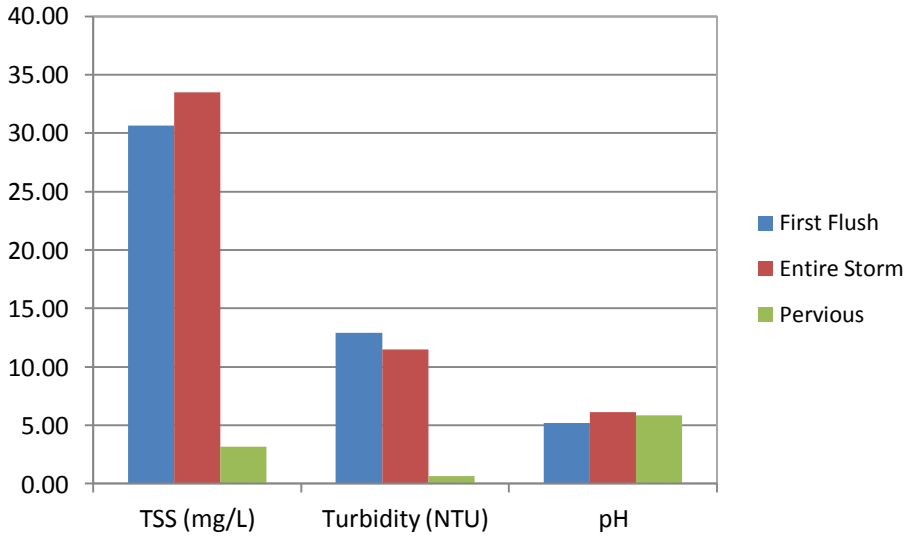

Figure 57. Control section weirs; water quality results of water sample collected on 07/29/2012

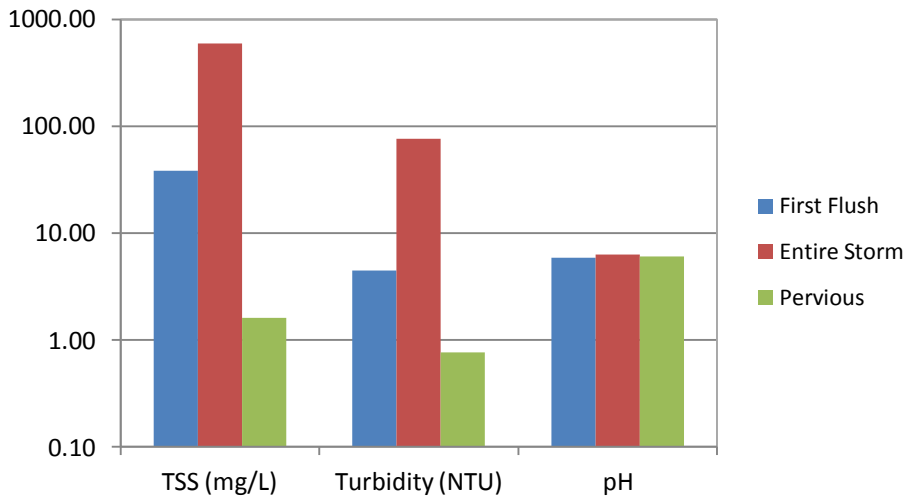

Figure 58. TX active weirs; water quality results of water sample collected on 07/29/2012

Table 17 provides the ion quantities for the construction water and Table 18 provides the ion quantities of the first stormwater sample picked up from the field in November 7th, 2012. Figure 59 is a typical chromatogram; however the sample depicted is the standard used for calibrating the IC. Appendix D provides the statistical analysis of the construction water samples. Appendix E provides the statistical analysis of the rainwater samples.

Table 17. Ion concentrations of construction water

	Ion Quantities (ppm), Averages of three replicates						
Sample	Fluoride	Chloride	Nitrite	Bromide	Nitrate	Phosphate	Sulfate
Ctrl Water	0.823	39.834	0.386	0.183	1.847	0.079	390.229
TX Water	0.866	39.619	-	0.229	3.727	0.551	380.893

Table 18. Ion concentrations of rainwater samples

	Ion Quantities (ppm), Averages of three replicates						
Sample	Fluoride	Chloride	Nitrite	Bromide	Nitrate	Phosphate	Sulfate
Ctrl Pervious	1.142	1.114	-	-	0.395	-	56.358
Ctrl Entire Strom	0.446	1.774	-	-	-	-	27.921
Ctrl First Flush	Too High	9.437	-	0.040	-	25.630	90.265
TX Pervious	2.270	1.412	-	-	7.114	0.034	326.099
TX Entire Storm	0.347	1.750	-	-	0.819	-	27.419
TX First Flush	0.292	1.860	-	0.003	-	0.005	29.147

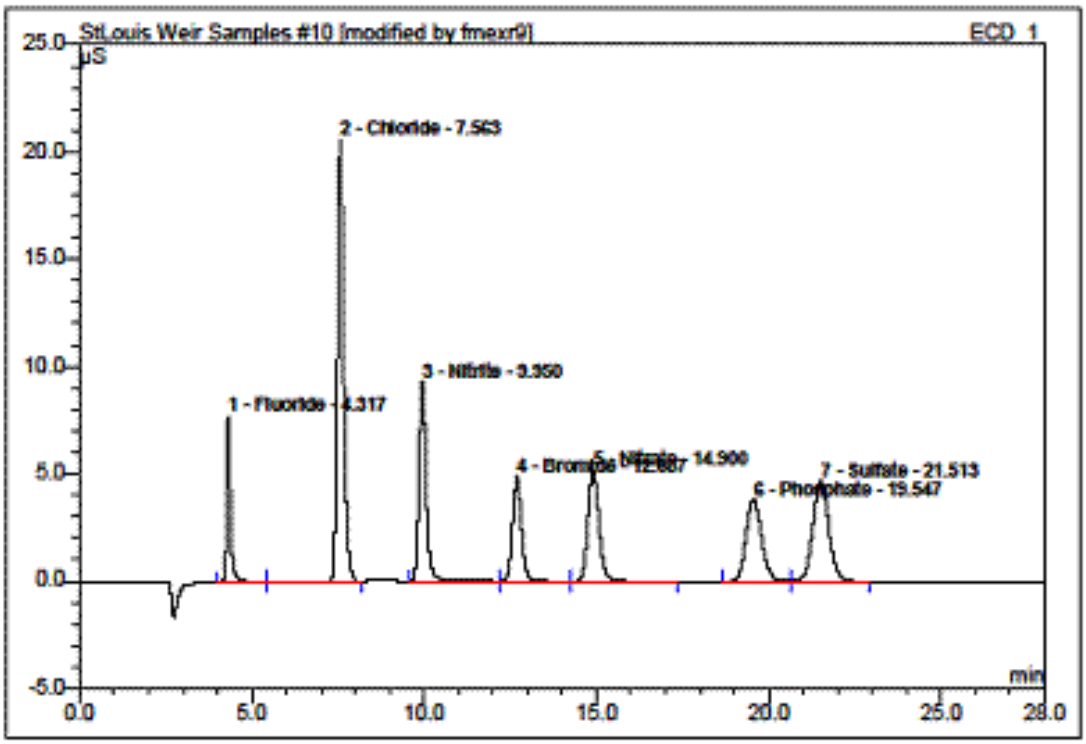

No.	Ret.Time min	Peak Name	Height µS	Area µS*min	Rel.Area %	Amount ppm	Type
1	4.32	Fluoride	7.688	1.049	6.66	1.990	BMb
2	7.56	Chloride	20.637	4.558	28.95	13.276	bMB
3	9.95	Nitrite	9.285	2.310	14.67	10.868	BM *
4	12.89	Bromide	4.857	1.475	9.37	9.604	M *
5	14.90	Nitrate	5.150	1.876	11.91	11.951	MB*
6	19.55	Phosphate	3.794	1.979	12.57	23.478	BM
7	21.51	Sulfate	4.654	2.498	15.87	12.037	MB
Total:			56.065	15.745	100.00	83.204	

Figure 59. Chromatogram for a standard used for calibration of the IC

CHAPTER 7

CONSTRUCTION CHALLENGES AND OBSERVATIONS

The research portions of this project were subject to scheduling, material procurement, constructability, and coordination amongst differing entities as persistent with typical construction and thus were also subject to the challenges that arose from these aspects of construction. However, due to the demand to meet the overall time requirements and to complete the project as mandated prior to construction, research scheduling was the most easily altered. This chapter discusses some of those challenges along with some observations.

Overall Timeframe of Research

The first major challenge encountered with the project included the delay of the construction of the shoulders of the highway which was essential to the research being conducted. The initial strategy was to complete this portion of the construction so as to determine tangible background information on the highway's water quality improving ability prior to major traffic flow. The initial arrangements were to provide the winter season of 2011 to the spring season of 2012 as background data, however the construction of the highway shoulders was not completed until the spring of 2012; the pervious concrete shoulders were paved in early May. This, along with a severe drought, had reduced any

possibility of background data, as the highway was opening for traffic only two months afterwards. This decreased the potential of capturing rain events and thus reduced the available data to compare water quality of a pavement with little to no traffic and one with typical traffic flow.

Power Supply

All of the data acquisition equipment that was installed was battery operated and connected to a power outlet installed within the vaults so as to recharge the batteries continuously. The battery packs for all of the equipment were meant to continue to collect data for a given amount of time depending on how many instruments were connected to them even if the power was disconnected for a short time. The issue that was present was the fact that the main power supply to the vault was never connected, and power was still not connected as of Spring 2013. This had diminished data collection as the batteries need to be removed and recharged on a continuous basis in order to remain operational, which was not feasible due to the distance of the site from the research team. This however was a fortunate predicament, as the vaults were flooded with water, which could have been a potentially dangerous situation.

Concrete Vaults

The vaults used for protecting the instruments and the power supply were much more heavy duty than required. The problem associated with the heavy duty vaults was the susceptibility for water infiltration, and the consequential water that was retained. Figure 60 depicts one of the two vaults used that was entirely flooded and the equipment floating

within it since there was no way to purge the water. The data logger was saved because of the container it was in which was floating and protected from the water infiltration. The other vault similarly did flood, however the water was expelled which introduced the rusting and corrosion of all of the equipment, as shown in Figure 61 and 62. The rust progressed to the point that the screws used to hold up the water sampler stand sheared off breaking off one of the legs and knocking down the equipment, Figure 63. As a comparison, an image of the equipment stand is provided in Figure 64, showing the water samplers standing upright. The vault that was rusted was the one housing the weather station, and the data logger was so severely damaged that the data could not be downloaded on to a computer. Thus this data is incomplete and insufficient to provide an adequate comparison between rainfall and the discharge of water from the pervious concrete shoulders. Furthermore, the water samplers which were meant to be installed upright, leaked battery fluid, possibly contaminating the water samples, as shown in Figure 62 previously. Along with the heavy duty vaults, the lids that were used were far too heavy to be easily managed by one individual, which presented a danger to anyone opening the vaults.

Figure 60. Instruments floating within vault due to flooding

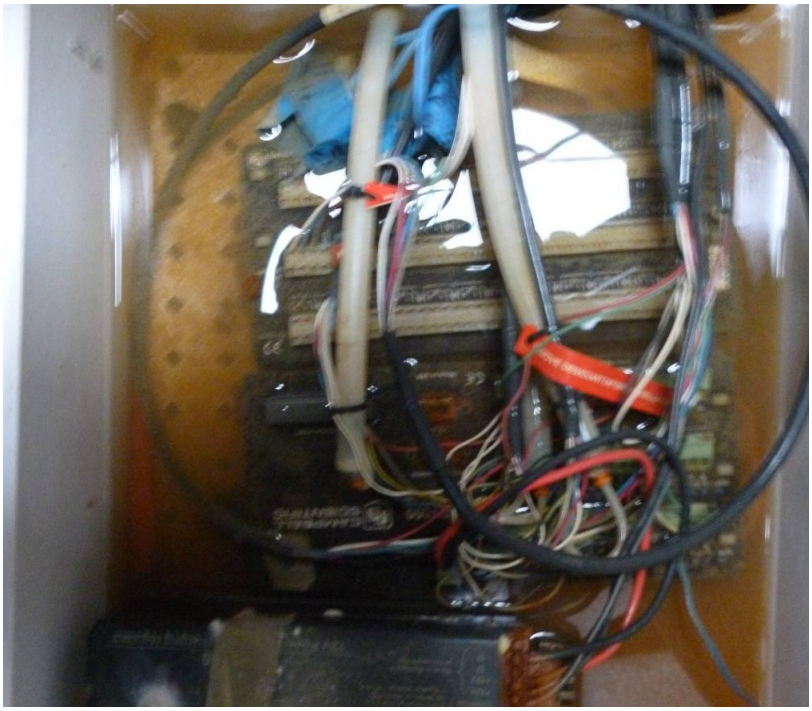

Figure 61. Instrument corrosion and battery leak due to flooding

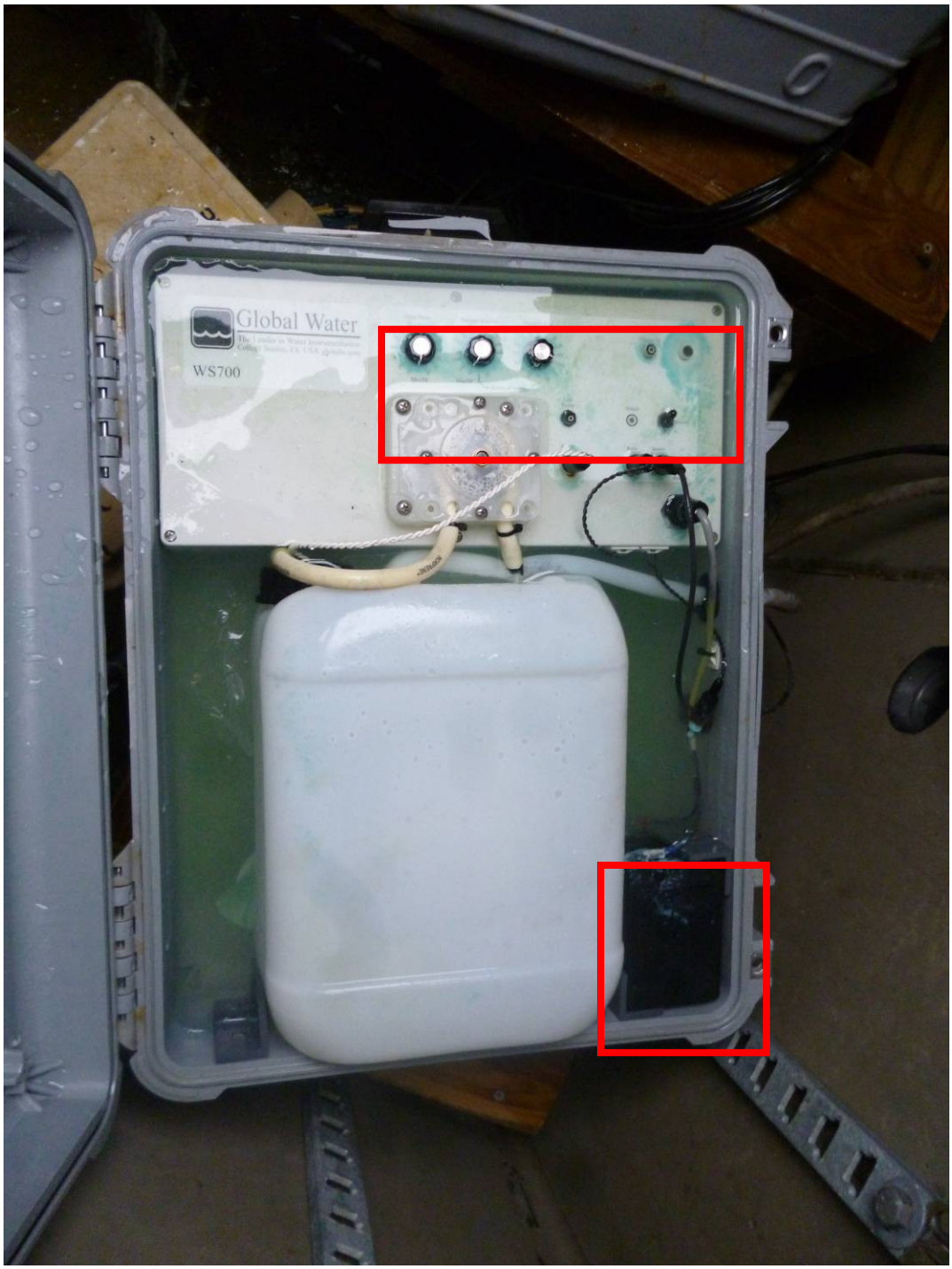

Figure 62. Flooding induced damage and battery corrosion to water samplers

Figure 63. Equipment knocked down due to the rusting of the mount screws.

Figure 64. Water sampler stand prior to rusting of mount screws

Pervious Concrete Shoulders

The pervious concrete was installed in early May 2012, and was constructed a few months prior to the completion of the project. In order to maintain the porosity of the pavement, it was necessary to protect the surface from debris after the concrete had set, including that associated with construction. However, visually the pavement seemed to be clogged prior to any rain event, as shown in Figure 65 and 66. To mitigate this, the concrete was cleaned using a vacuum truck and pressurized washing, depicted in Figures 67-70. After this, the pervious concrete was protected using sandbags and hay bales around the perimeter of the pervious concrete shoulders.

Figure 65. Clogged pervious concrete shoulders prior to vacuuming

Figure 66. Close-up of clogged pervious concrete shoulders

Figure 67. Water pooling on the pervious concrete pavement

Figure 68. Vacuuming pervious concrete shoulders

Figure 69. Close-up of vacuuming/washing operation

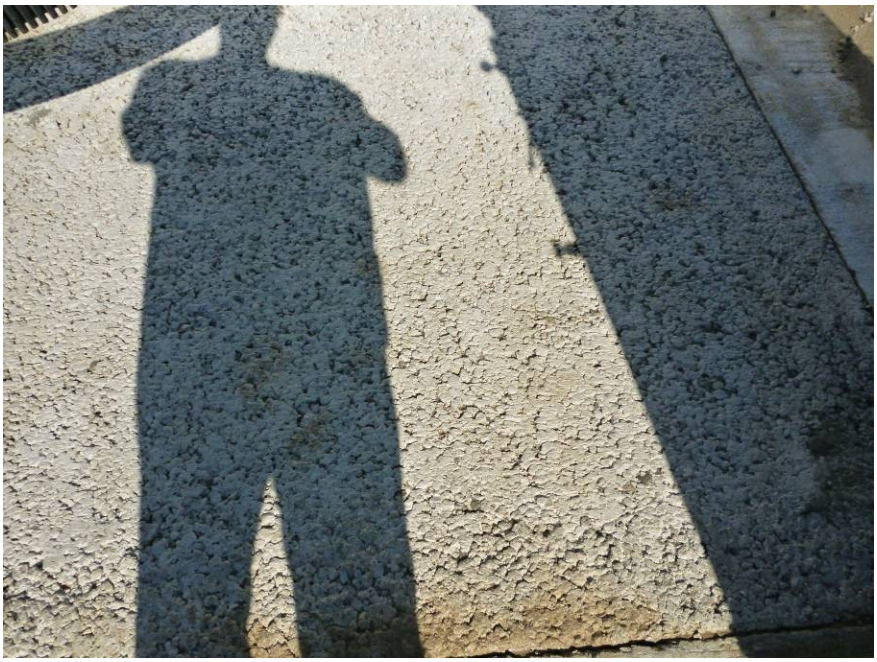

Figure 70. Pervious concrete shoulders after vacuuming

Upon the completion of the vacuuming operation, the rate of infiltration was being determined as described in the "Methods and Instrumentation Process" chapter above. However, the rate of infiltration was very low, and further possibilities were being discussed as to what the issue might be. The MoDOT office had sent to obtain core samples of the concrete and sent them for analysis by the research team. The percent voids of the core samples were determined, as were the ratio of materials used using image analysis, Figure 71 and 72. It was determined from this that the concrete mix design was not appropriate as the concrete had a high cementitious material ratio, as indicated by the results provided in Table 19. This adversely affected the porosity of the concrete, as the cementitious material simply filled in the voids, causing the concrete to be impermeable. This meant that that the pervious

concrete was not as pervious as specified, and would need reconstruction for functionality. As of late February 2013, arrangements have been made to reconstruct the shoulders in the summer of 2013.

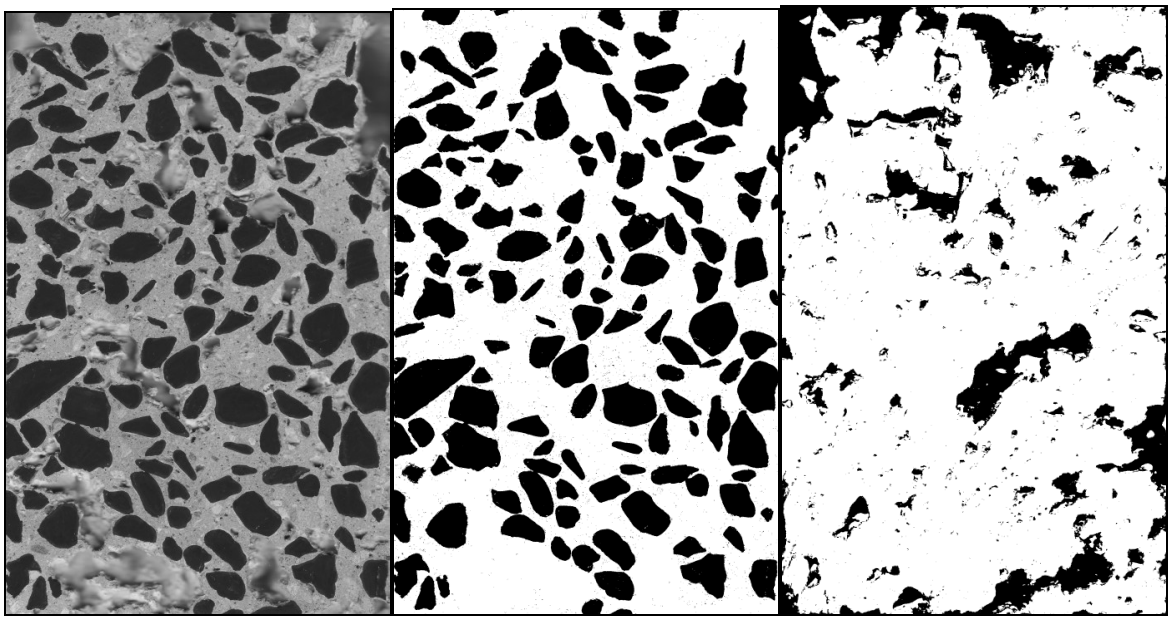

Figure 71. TX Active Image analysis of cored samples, cross-section of sample with aggregates black (left), aggregate volume (middle), voids black on mirrored surface (right)

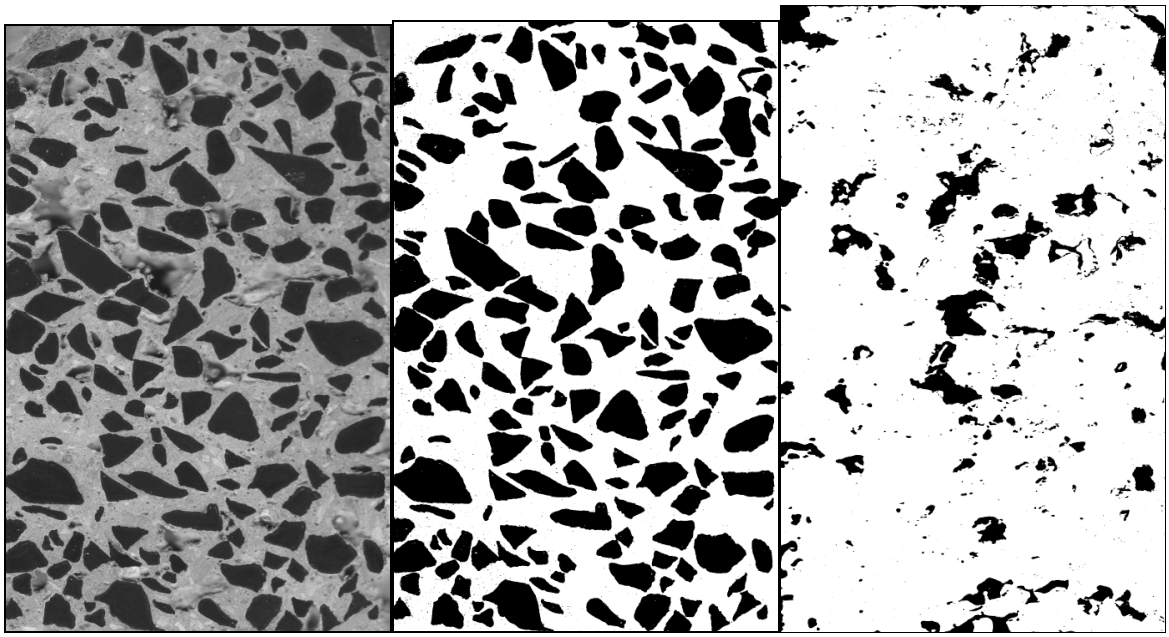

Figure 72. PCPC image analysis of cored samples, cross-section of sample with aggregates black (left), aggregate volume (middle), voids black on mirrored surface (right)

Table 19. Material volumes of TX Active core, determined with image analysis

	Design	TXPC Actual	PCPC Actual
Aggregate Volume	46.1%	36.71%	39.45%
Mortar Volume	29.6%	46.16%	49.88%
Voids Volume	24.3%	17.14%	10.67%
Mortar/Agg Ratio	0.64	1.26	1.26

Weather Conditions

Though this is considered part of natural conditions, the year of 2012 presented the Midwest with extreme drought that had prevented any analysis on stormwater, as there were no rain events to analyze. Appendix F provides a map of the state of Missouri to depict the effects of the drought as of September 18, 2012. This data shows that from mid June to mid September, nearly one third of the state of Missouri was witnessing severe to extreme drought, as was the location of the highway.

Best Practices and Lessons Learned

Though many of these challenges that were observed are common with construction practices, some notes and suggestions were made for future work with this technology. Ultimately, the overall communication between all participating parties is compulsory for proper execution of any project. Communication between all parties was the key to successful execution of problem solving of onsite issues such as vacuuming the pervious concrete and then protecting the shoulders from debris. With more communication of this sort, fewer problems would have been apparent as such problems would have been dealt with immediately upon recognition.

Best practices for future projects dictate that instrumentation be waterproofed and situated so as to avoid any mishaps caused by unforeseen failures. This includes mounting sensitive equipment in water tight panels, mounting heavy equipment and equipment filled with water on ground level to avoid tipping/leaking and providing means for desiccating the vaults. Forecasting possible problems would have also reduced the impact of the problems

that were observed as well. For example, anticipating the potential for vault flooding would have lead to better management of data collection, as well as the preparation of alternatives to power supply to minimize the downtime of the equipment.

CHAPTER 8

SUMMARY AND CONCLUSIONS

The results provided in the previous section are used to attain the overall objective of the research; to explicitly determine the feasibility and advantages of pervious concrete and photocatalytic concrete in highways. This section provides a summary of the major findings and provides the conclusions that were perceived.

Laboratory Simulation

The laboratory simulation did in fact prove the reactivity of the TX Active cements. However, the results were expected to prove the formation of nitrate ions, but proved the formation of nitrite ions instead. This could potentially be associated with ambient humidity levels. The TXPC had higher voids, which may have increased the reactivity of the sample.

Two-Lift Results

The compressive strength of concrete cylinders is a common and simple way to check consistency of the concrete. Though the top lift certainly meets strength criteria on a highway pavement, and the bottom lift far surpasses this as well, it would be expected that the top lift is stronger than the bottom lift. As this is the surface that is exposed to environmental conditions, the durability and strength of the top lift is typically greater than the bottom lift.

This does not necessarily affect the results pertinent to this study; however, it is a notable finding.

Subbase Characteristics

From the results of the subbase material testing, it was determined that the subbase was well graded, as depicted by the gradation curve, and the coefficient of uniformity was greater than four, and the coefficient of curvature was between one and three. This was assumed to be adverse to water storage, as the subbase has fewer voids than an open graded subbase. The fewer voids equates to a smaller volume of potential storage space. However, this does not necessarily reflect upon a poor design, as this may be a criteria set by presiding agencies. In fact, the data from the data logger showed that the water in the subbase was not retained for long periods of time. Furthermore, the subbase being well graded does not imply that there is little storage space, it just indicative of less storage capacity than an open graded base.

Albedo of New Pavement

The albedo of all of the new pavements ranged from 29%-33%, for both the photocatalytic, pervious, and conventional concrete. This was not expected, as the photocatalytic concrete is significantly lighter in color, especially when newly placed or when moist. The photocatalytic concrete did have a slightly higher albedo than the conventional concrete, and the pervious had lower albedo than the conventional. It was expected that the photocatalytic concrete would in fact have a higher albedo, but the lower albedo of the pervious concrete is indicative of soil deposited on the surface of the pavement

even with the measures in place to prevent clogging. It is noteworthy that the entire pavement was sullied due to the construction process, and it is expected that the albedo of the photocatalytic concrete and pervious concrete would increase upon the first rain event.

On-Site Conditions

The weather data depicts a warmer and dryer summer and fall than the average conditions for the same time period. This had led to fewer storms being collected, but this was not a severe issue due to other dictating incidents, such as the vault malfunction.

The data downloaded from the data logger indicates that there were occasional storms throughout the months when the data logger had power. The figures showing the data from the pressure transducers depicted that early September had the largest storm captured by the logger. Despite the high amount of fines in the subbase, this data showed that the water drained quickly from the subbase. This is an important find as the subbase material typically would not qualify for structural stormwater management systems. The data showed that the largest flow from the mainline weir box was nearly 0.605 cubic feet per second. The largest flow from the pervious weir box was nearly 0.077 cubic feet per second. This is indicative of an issue with the pervious concrete shoulders, and suggests that the concrete may have a low permeability. The weir collecting the runoff from the mainline pavement never fully drained from the first observed storm, and that the pervious concrete weir eventually did clog as well. Thus in order to determine the volume of water through the sections, the final height of the water needs to be subtracted from height just prior to the spike indicating a storm.

The temperature of the water indicates that the water within the aggregate subbase was more stable and less susceptible to ambient temperatures. This is expected, since the pervious concrete acts as a thermal insulator for the subbase. The temperature fluctuations of the weir boxes indicate that the weir temperature was subject to temperature peaks and drops associated with the heat from the sun. These fluctuations also suggest that the weir box collecting runoff from the pervious concrete shoulders was under the heat of the sun more, which was in fact the case, as there is more tree cover around the mainline weir box.

The temperature sensors fluctuated according to expectation, raising in the day and dropping at night. The surface temperature fluctuates more than the rest of the temperatures as the surface is exposed to the sun, while the remaining subsurface temperatures were steadier. The temperatures recorded by the sensors a foot below the mainline pavement, in the middle of the mainline concrete, the interface of the aggregate subbase with the pervious concrete, and in the middle of the pervious concrete showed comparable trends, with the exception of a few peaks associated with rainwater infiltrating the shoulders and slightly decreasing the temperatures measured within the middle of the pervious concrete and within the aggregate subbase beneath the pervious concrete. Notably, this indicates that water draws heat from the pervious concrete and subbase.

Water Quality Results

The higher pH in the construction water indicated that the pavement had a high pH; the results, however, do not definitely conclude if the differing cements affected the overall pH. There seemed to be a larger quantity of suspended solids in the control section than in

the test. This could potentially be due to the ongoing construction further south of the sections, but closer to the control section. The water quality of the rain water samples collected indicated that the pH was lower than that of water, most likely due to the acidity (low pH) of the battery fluid. There was a larger quantity of suspended solids rain water samples of the test section than in the control section. This could be resultant of the landscaping efforts near the interchange that were ongoing after the construction was completed, north of the test section. he ion concentrations show that fluoride is common to both the control section as well as the photocatalytic, however they were significantly different from one another. There was a higher concentration of fluorides coming from the pervious concrete than the mainline concrete, and the photocatalytic concrete had higher concentrations. Chloride concentrations when compared to their similar collection points are all significantly different. The control samples first flush is a suspected outlier, as this is the only section that is so high in chlorides. Nitrites and bromides were uncommon for both sections in both the pervious and mainline pavements. Phosphates were as well, except for the control section first flush, which seems to indicate, along with the chloride concentrations, that there may have been a contamination of the water sample. Nitrates and sulfates were high in the photocatalytic concrete, which is expected, as the reaction of the TX Active cement with NO_x and SO_x results in these ions. It was also proven from the higher nitrate concentrations that the pervious concrete was more reactive than the mainline, which is also expected.

The difference between the photocatalytic results from the construction water and the photocatalytic mainline stormwater could indicate the decrease in reactivity of the photocatalytic cement, as there is a decrease in the amount of nitrates present. However, this data cannot be verified with these results alone as the water from the construction process was non-potable water, not rainwater. Furthermore, one data point is not adequate enough to reach this inference.

Future work should include continued data collection on the highway in order to more surely determine the efficacy of the technology. Further assessment on pervious concrete shoulders should be conducted, in order to determine the benefits of it for storm drainage purposes. Future laboratory assessment should include determining the effects of environmental constraints on the reactivity of the TX Active cements, including the role of humidity on the reactivity, and the role of daylong rain events where there is the potential for cloud breaks.

APPENDIX A

WEIR BOX CALIBRATION

Bottom of V:	22.1 (cm)	V-notch Angle:	30°
height (cm)	head (cm)	Venturi Reading (cm)	Weir Reading (cm)
28.42	6.32	0.01722	0.01495
28.76	6.66	0.021085	0.01694
30.01	7.91	0.02277	0.02558
32.49	10.39	0.0385	0.0494
34.89	12.79	0.07747	0.082
35.94	13.84	0.1068	0.0992
38.71	16.61	0.1535	0.1555
39.07	16.97	0.1789	0.1639
39.95	17.85	0.198	0.1855
40.18	18.08	0.202	0.1915

APPENDIX B

FLUME DATA

PCPC											
Run	Left Venturi	Right Venturi	Venturi H (ft of water)	Infiltration V-notch (mm)	Infiltration V-notch (inches)	Tailbox V-notch (mm)	Tailbox V-notch (in)	Venturi Flow Rate (cfs)	Infil. Flowrate	Overflow flowrate	Combined flowrate
1	0.1	0.1	0.0325	131	2.677	100	3.503937008	0.0172	0.0132	0.0240	0.0372
2	0.95	1	0.316875	140	3.031	188	6.968503937	0.0538	0.0180	0.1340	0.1521
3	1.6	1.7	0.53625	140	3.031	214	7.992125984	0.0699	0.0180	0.1888	0.2068
4	2.1	2.2	0.69875	141	3.071	228	8.543307087	0.0798	0.0186	0.2231	0.2417
5	2.9	3	0.95875	141	3.071	237	8.897637795	0.0935	0.0186	0.2469	0.2655
TXPC											
Run	Left Venturi	Right Venturi	Venturi H (ft of water)	Infiltration V-notch (mm)	Infiltration V-notch (inches)	Tailbox V-notch (mm)	Tailbox V-notch (in)	Venturi Flow Rate (cfs)	Infil. Flowrate (cfs)	Overflow flowrate (cfs)	Combined flowrate (cfs)
1	0.25	0.25	0.08125	151	3.465	0	0	0.0272	0.0252	0.0000	0.0252
2	0.6	0.7	0.21125	171	4.252	0	0	0.0439	0.0420	0.0000	0.0420
3	1.3	1.4	0.43875	185	4.803	120	4.291338583	0.0633	0.0569	0.0399	0.0968
4	2.8	2.9	0.92625	192	5.079	147	5.354330709	0.0919	0.0655	0.0694	0.1348
5	5.2	5.3	1.70625	199	5.354	212	7.913385827	0.1247	0.0747	0.1842	0.2589

APPENDIX C

STATISTICAL ANALYIS OF LAB SAMPLE WATER

General Linear Model: Fluoride, Chloride, ... versus Water Sample

```
Factor        Type   Levels  Values
Water Sample  fixed       2  Ctrl DI Effluent, TX DI Effluent


Analysis of Variance for Fluoride, using Adjusted SS for Tests

Source        DF    Seq SS    Adj SS    Adj MS     F      P
Water Sample   1  0.000129  0.000129  0.000129  0.07  0.810
Error          4  0.007819  0.007819  0.001955
Total          5  0.007948


S = 0.0442125   R-Sq = 1.62%   R-Sq(adj) = 0.00%


Analysis of Variance for Chloride, using Adjusted SS for Tests

Source        DF    Seq SS    Adj SS    Adj MS     F      P
Water Sample   1  0.002042  0.002042  0.002042  0.53  0.508
Error          4  0.015508  0.015508  0.003877
Total          5  0.017551


S = 0.0622659   R-Sq = 11.64%   R-Sq(adj) = 0.00%


Analysis of Variance for Nitrite, using Adjusted SS for Tests

Source        DF     Seq SS     Adj SS     Adj MS      F      P
Water Sample   1  0.0010613  0.0010613  0.0010613  22.92  0.009
Error          4  0.0001852  0.0001852  0.0000463
Total          5  0.0012465


S = 0.00680429   R-Sq = 85.14%   R-Sq(adj) = 81.43%


Analysis of Variance for Nitrate, using Adjusted SS for Tests

Source        DF   Seq SS   Adj SS   Adj MS     F      P
```

```
Water Sample   1  0.00464  0.00464  0.00464  0.07  0.805
Error          4  0.26776  0.26776  0.06694
Total          5  0.27240


S = 0.258726   R-Sq = 1.70%   R-Sq(adj) = 0.00%


Analysis of Variance for Phosphate, using Adjusted SS for Tests

Source        DF  Seq SS  Adj SS  Adj MS     F      P
Water Sample   1  1.0048  1.0048  1.0048  7.24  0.055
Error          4  0.5552  0.5552  0.1388
Total          5  1.5600


S = 0.372548   R-Sq = 64.41%   R-Sq(adj) = 55.52%


Analysis of Variance for Sulfate, using Adjusted SS for Tests

Source        DF   Seq SS   Adj SS   Adj MS       F      P
Water Sample   1  0.69224  0.69224  0.69224  376.21  0.000
Error          4  0.00736  0.00736  0.00184
Total          5  0.69960


S = 0.0428957   R-Sq = 98.95%   R-Sq(adj) = 98.68%
```

Results for: Worksheet 11

ANOVA: Fluoride, Chloride, ... versus Water Sample

```
* WARNING * Not all response variables have the same missing value pattern. You
            would get different univariate results if you ran this command
            separately for each of these response variables. See the Help topic
            'missing values' for details.


Factor        Type   Levels  Values
Water Sample  fixed       2  Ctrl UV Effluent, TX UV Effluent


Analysis of Variance for Fluoride

Source        DF        SS        MS      F      P
Water Sample   1  0.023291  0.023291  74.51  0.003
Error          3  0.000938  0.000313
Total          4  0.024229


S = 0.0176806   R-Sq = 96.13%   R-Sq(adj) = 94.84%


Analysis of Variance for Chloride
```

Source	DF	SS	MS	F	P
Water Sample	1	0.10026	0.10026	75.88	0.003
Error	3	0.00396	0.00132		
Total	4	0.10422			

S = 0.0363493 R-Sq = 96.20% R-Sq(adj) = 94.93%

Analysis of Variance for Nitrite

Source	DF	SS	MS	F	P
Water Sample	1	0.00013911	0.00013911	**	
Error	3	0.00000241	0.00000080		
Total	4	0.00014151			

** Denominator of F-test is zero or undefined.

S = 0.000895669 R-Sq = 98.30% R-Sq(adj) = 97.73%

Analysis of Variance for Nitrate

Source	DF	SS	MS	F	P
Water Sample	1	0.00002708	0.00002708	0.33	0.605
Error	3	0.00024456	0.00008152		
Total	4	0.00027164			

S = 0.00902893 R-Sq = 9.97% R-Sq(adj) = 0.00%

Analysis of Variance for Phosphate

Source	DF	SS	MS	F	P
Water Sample	1	0.0343	0.0343	0.09	0.785
Error	3	1.1571	0.3857		
Total	4	1.1915			

S = 0.621056 R-Sq = 2.88% R-Sq(adj) = 0.00%

Analysis of Variance for Sulfate

Source	DF	SS	MS	F	P
Water Sample	1	0.82984	0.82984	47.92	0.006
Error	3	0.05195	0.01732		
Total	4	0.88178			

S = 0.131590 R-Sq = 94.11% R-Sq(adj) = 92.15%

APPENDIX D

STATISTICAL ANALYIS OF CONSTRUCTION WATER

General Linear Model: Fluoride, Chloride, ... versus Water Sample

```
Factor        Type   Levels  Values
Water Sample  fixed       2  Xtruction Ctrl, Xtruction TX


Analysis of Variance for Fluoride, using Adjusted SS for Tests

Source        DF     Seq SS     Adj SS     Adj MS     F      P
Water Sample   1  0.0027221  0.0027221  0.0027221  9.81  0.035
Error          4  0.0011102  0.0011102  0.0002776
Total          5  0.0038324


S = 0.0166599   R-Sq = 71.03%   R-Sq(adj) = 63.79%


Analysis of Variance for Chloride, using Adjusted SS for Tests

Source        DF    Seq SS    Adj SS    Adj MS      F      P
Water Sample   1  0.069295  0.069295  0.069295  20.15  0.011
Error          4  0.013755  0.013755  0.003439
Total          5  0.083050


S = 0.0586411   R-Sq = 83.44%   R-Sq(adj) = 79.30%


Analysis of Variance for Nitrite, using Adjusted SS for Tests

Source        DF   Seq SS   Adj SS   Adj MS         F      P
Water Sample   1  0.22403  0.22403  0.22403  67244.04  0.000
Error          4  0.00001  0.00001  0.00000
Total          5  0.22405


S = 0.00182529   R-Sq =  99.99%   R-Sq(adj) = 99.99%


Analysis of Variance for Bromide, using Adjusted SS for Tests
```

Source	DF	Seq SS	Adj SS	Adj MS	F	P
Water Sample	1	0.003192	0.003192	0.003192	0.93	0.390
Error	4	0.013734	0.013734	0.003433		
Total	5	0.016926				

S = 0.0585960 R-Sq = 18.86% R-Sq(adj) = 0.00%

Analysis of Variance for Nitrate, using Adjusted SS for Tests

Source	DF	Seq SS	Adj SS	Adj MS	F	P
Water Sample	1	5.2984	5.2984	5.2984	18000.56	0.000
Error	4	0.0012	0.0012	0.0003		
Total	5	5.2996				

S = 0.0171565 R-Sq = 99.98% R-Sq(adj) = 99.97%

Analysis of Variance for Phosphate, using Adjusted SS for Tests

Source	DF	Seq SS	Adj SS	Adj MS	F	P
Water Sample	1	0.33446	0.33446	0.33446	575.78	0.000
Error	4	0.00232	0.00232	0.00058		
Total	5	0.33678				

S = 0.0241015 R-Sq = 99.31% R-Sq(adj) = 99.14%

Analysis of Variance for Sulfate, using Adjusted SS for Tests

Source	DF	Seq SS	Adj SS	Adj MS	F	P
Water Sample	1	130.75	130.75	130.75	1803.78	0.000
Error	4	0.29	0.29	0.07		
Total	5	131.04				

S = 0.269234 R-Sq = 99.78% R-Sq(adj) = 99.72%

APPENDIX E

STATISTICAL ANALYSIS OF RAINWATER SAMPLES

General Linear Model: Sulfate, Fluoride, ... versus Water Sample Per

```
Factor                 Type   Levels  Values
Water Sample Pervious  fixed       2  Ctrl Pervious, TX Pervious


Analysis of Variance for Sulfate, using Adjusted SS for Tests

Source                 DF  Seq SS  Adj SS  Adj MS         F      P
Water Sample Pervious   1  138765  138765  138765  45638.44  0.000
Error                   4      12      12       3
Total                   5  138777


S = 1.74371   R-Sq = 99.99%   R-Sq(adj) = 99.99%


Analysis of Variance for Fluoride, using Adjusted SS for Tests

Source                 DF  Seq SS  Adj SS  Adj MS         F      P
Water Sample Pervious   1  1.9074  1.9074  1.9074  32851.17  0.000
Error                   4  0.0002  0.0002  0.0001
Total                   5  1.9077


S = 0.00761993   R-Sq = 99.99%   R-Sq(adj) = 99.98%


Analysis of Variance for Chloride, using Adjusted SS for Tests

Source                 DF  Seq SS  Adj SS  Adj MS           F      P
Water Sample Pervious   1  57.320  57.320  57.320  2228741.01  0.000
Error                   4   0.000   0.000   0.000
Total                   5  57.320


S = 0.00507132   R-Sq = 100.00%   R-Sq(adj) = 100.00%


Analysis of Variance for Nitrate, using Adjusted SS for Tests

Source                 DF  Seq SS  Adj SS  Adj MS          F      P
```

```
Water Sample Pervious   1  92.930  92.930  92.930  897929.80  0.000
Error                   4   0.000   0.000   0.000
Total                   5  92.930


S = 0.0101732   R-Sq = 100.00%   R-Sq(adj) = 100.00%
```

General Linear Model: Fluoride ES, Chloride ES, ... versus Water Sample

```
Factor           Type   Levels  Values
Water Sample ES  fixed       2  Ctrl Entire Strom, TX Entire Storm


Analysis of Variance for Fluoride ES, using Adjusted SS for Tests

Source           DF    Seq SS    Adj SS    Adj MS     F      P
Water Sample ES   1  0.000859  0.000859  0.000859  0.50  0.520
Error             4  0.006927  0.006927  0.001732
Total             5  0.007786


S = 0.0416142   R-Sq = 11.04%   R-Sq(adj) = 0.00%


Analysis of Variance for Chloride ES, using Adjusted SS for Tests

Source           DF   Seq SS   Adj SS   Adj MS        F      P
Water Sample ES   1  0.26083  0.26083  0.26083  3224.55  0.000
Error             4  0.00032  0.00032  0.00008
Total             5  0.26116


S = 0.00899389   R-Sq = 99.88%   R-Sq(adj) = 99.85%


Analysis of Variance for Sulfate ES, using Adjusted SS for Tests

Source           DF  Seq SS  Adj SS  Adj MS     F      P
Water Sample ES   1  169.50  169.50  169.50  7.10  0.056
Error             4   95.54   95.54   23.88
Total             5  265.04


S = 4.88710   R-Sq = 63.95%   R-Sq(adj) = 54.94%
```

General Linear Model: Fluoride FF, Chloride FF, ... versus Water Sample

```
Factor           Type   Levels  Values
Water Sample FF  fixed       2  Ctrl First Flush, TX First Flush


Analysis of Variance for Fluoride FF, using Adjusted SS for Tests

Source           DF   Seq SS   Adj SS   Adj MS      F      P
Water Sample FF   1  0.12822  0.12822  0.12822  91.68  0.001
```

```
Error             4  0.00559  0.00559  0.00140
Total             5  0.13381


S = 0.0373975   R-Sq = 95.82%   R-Sq(adj) = 94.77%


Analysis of Variance for Chloride FF, using Adjusted SS for Tests

Source           DF   Seq SS  Adj SS  Adj MS      F      P
Water Sample FF   1   86.112  86.112  86.112  23.38  0.008
Error             4   14.735  14.735   3.684
Total             5  100.847


S = 1.91929   R-Sq = 85.39%   R-Sq(adj) = 81.74%


Analysis of Variance for Bromide FF, using Adjusted SS for Tests

Source           DF     Seq SS     Adj SS     Adj MS     F      P
Water Sample FF   1  0.0008568  0.0008568  0.0008568  3.05  0.156
Error             4  0.0011242  0.0011242  0.0002811
Total             5  0.0019810


S = 0.0167648   R-Sq = 43.25%   R-Sq(adj) = 29.06%


Analysis of Variance for Phosphate FF, using Adjusted SS for Tests

Source           DF  Seq SS  Adj SS  Adj MS         F      P
Water Sample FF   1  984.97  984.97  984.97  77805.26  0.000
Error             4    0.05    0.05    0.01
Total             5  985.02


S = 0.112514   R-Sq =  99.99%   R-Sq(adj) = 99.99%


Analysis of Variance for Sulfate FF, using Adjusted SS for Tests

Source           DF  Seq SS  Adj SS  Adj MS         F      P
Water Sample FF   1  5603.2  5603.2  5603.2  22013.54  0.000
Error             4     1.0     1.0     0.3
Total             5  5604.2


S = 0.504512   R-Sq = 99.98%   R-Sq(adj) = 99.98%
```

APPENDIX F

DROUGHT DATA

U.S. Drought Monitor

September 18, 2012
Valid 7 a.m. EST

Missouri

Drought Conditions (Percent Area)

	None	D0-D4	D1-D4	D2-D4	D3-D4	D4
Current	0.00	100.00	100.00	84.55	16.90	0.00
Last Week (09/11/2012 map)	0.00	100.00	100.00	89.68	25.20	0.78
3 Months Ago (06/19/2012 map)	1.30	98.70	86.71	31.82	8.06	0.00
Start of Calendar Year (12/27/2011 map)	95.48	4.52	0.00	0.00	0.00	0.00
Start of Water Year (09/27/2011 map)	55.19	44.81	22.45	8.65	0.00	0.00
One Year Ago (09/13/2011 map)	41.12	58.88	26.36	8.56	0.00	0.00

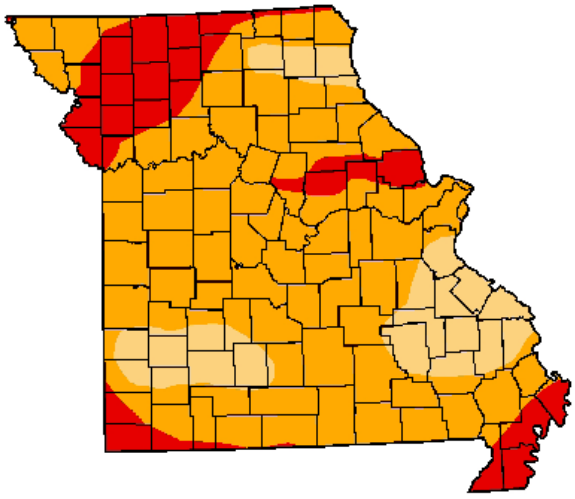

Intensity:

- *D0 Abnormally Dry*
- *D1 Drought - Moderate*
- *D2 Drought - Severe*
- *D3 Drought - Extreme*
- *D4 Drought - Exceptional*

The Drought Monitor focuses on broad-scale conditions. Local conditions may vary. See accompanying text summary for forecast statements.

http://droughtmonitor.unl.edu

Released Thursday, September 20, 2012
David Simeral, Western Regional Climate Center

REFERENCES

ASTM Standard C29M, 2009, "Standard Test Method for Bulk Density ("Unit Weight") and Voids in Aggregate," *ASTM International*, West Conshohocken, PA, DOI: 10.1520/C0029_C0029M-09. www.astm.org.

ASTM Standard C31M, 2012, "Standard Practice for Making and Curing Concrete Test Specimens in the Field," *ASTM International*, West Conshohocken, PA, DOI: 10.1520/C0031_C0031M-12. www.astm.org.

ASTM Standard C39M, 2012, "Standard Test Method for Compressive Strength of Cylindrical Concrete Specimens," *ASTM International*, West Conshohocken, PA, DOI: 10.1520/C0039_C0039M-12A. www.astm.org.

ASTM Standard C127, 2012, "Standard Test Method for Density, Relative Density (Specific Gravity), and Absorption of Coarse Aggregate1" *ASTM International*, West Conshohocken, PA, DOI: 10.1520/C0127-12. www.astm.org.

ASTM Standard C136, 2006, "Standard Test Method for Bulk Density ("Unit Weight") and Voids in Aggregate," *ASTM International*, West Conshohocken, PA, DOI: 10.1520/C0136-06. www.astm.org.

ASTM Standard C1701M, 2009, "Standard Test Method for Infiltration Rate of In Place Pervious Concrete," *ASTM International*, West Conshohocken, PA, DOI: 10.1520/C1701_C1701M-09. www.astm.org.

ASTM Standard C1754M, 2012, "Standard Test Method for Density and Void Content of Hardened Pervious Concrete," *ASTM International*, West Conshohocken, PA, DOI: 10.1520/C1754_C1754M-12. www.astm.org.

ASTM Standard D1241, 2007, "Standard Specification for Materials for Soil-Aggregate Subbase, Base, and Surface Courses," *ASTM International*, West Conshohocken, PA, DOI: 10.1520/D1241-07. www.astm.org.

ASTM Standard E1918, 2006, "Standard Test Method for Measuring Solar Reflectance of Horizontal and Low-Sloped Surfaces in the Field," *ASTM International*, West Conshohocken, PA, DOI: 10.1520/E1918-06. www.astm.org.

Bentz, Dale, and Weiss, Jason. "Internal Curing: A 2010 State-of-the-Art Review." *National Institute of Standards and Technology* (2010).

Cable, James and Daniel Frentress. "Two-Lift Portland Cement Concrete Pavements to Meet Public Needs." *Center for Portland Cement Concrete Pavement Technology* (2004).

Castro, Javier, Schlitter, John, Henkensiefken, Ryan, Nantung, Tommy, & Weiss, Jason. "Internal Curing: Engineering Concrete for an Improved Service Life." Paper presented at American Concrete Pavement Association, Kansas City, MO, (2012).

Chen, Jun, Shi-cong Kou and Chi-Sun Poon. "Hydration and Properties of Nano-TiO_2 Blended Cement Composites." *Cement and Concrete Properties* 34 no. 5 (2012): 642-649.

"Climatology and Weather Records." N.p., 14 Jan. 2013. Web. 26 Apr. 2013. <http://www.crh.noaa.gov/lsx/?n=cli_archive>.

Dylla, Heather, Marwa Hassan, Marion Schmitt, Tyson Rupnow and Mohammad Louay. "Laboratory Investigation of the Effect of Mixed Nitrogen Dioxide and Nitrogen Oxide Gases on Titanium Dioxide Photocatalytic Efficiency in Concrete Pavements." *Journal of Materials in Civil Engineering* 23 (2011): 1087-1093.

Dylla, Heather, Marwa Hassan, Marion Schmitt, Tyson Rupnow, Louay Mohammad and Earle Wright. "Effects of Roadway Contaminants on Titanium Dioxide Photodegradation of Nitrogen Oxides."*Transportation Research Record: Journal of the Transportation Research Board* no. 2240 (2011): 22-29.

Fujishima, Akira and Xintong Zhang. "Titanium Dioxide Photocatalysis: Present Situation and Future Approaches." *Comptes Rendus Chimie* 9 no. 5-6 (2005): 750-760.

Kevern, John, Chris Farney. "Reducing Curing Requirements for Pervious Concrete with a Superabsorbent Polymer for Internal Curing." *Transportation Research Record: Journal of the Transportation Research Board* no. 2290 (2012): 115-121.

King, Gregory, Adam Bruetsch, John Kevern. "Slip-related characterization of gait kinetics: Investigation of pervious concrete as a slip-resistant walking surface." *Safety Science* 57, (2013): 52-59.

Hall, Kathleen, Dan Dawood, Suneel Vanikar, Robert Tally, Jr., Tom Cackler, Angel Correa, Peter Deem, James Duit, Georgene Geary, Andrew Gisi, Amir Hanna, Steven Kosmatka, Robert Rasmussen, Shiraz Tayabji, and Gerald Voigt. "Long-Life Concrete Pavements in Europe and Canada." *International Technology Scanning Program.* (2007). U.S. Department of Transportation: Federal Highway Administration.

Hassan, Marwa, Heather Dylla, Louay Mohammad and Tyson Rupnow. "Evaluation of the Durability of Titanium Dioxide Photocatalyst Coating for Concrete Pavement." *Construction and Building Materials* 24 (2010): 1456-1461.

Hassan, Marwa, Heather Dylla, Louay Mohammad and Tyson Rupnow. "Methods for the Application of Titanium Dioxide Coatings to Concrete Pavement."*International Journal of Pavement Research and Technology* 5 no. 1 (2012): 12-20.

Kosmatka, Steven, Beatrix Kerkhoff, and William Panarese. *Design and Control of Concrete Mixtures*. 15th Edition. Skokie, Illinois: Portland Cement Association, (2003).

Michigan Concrete Association. Pervious Concrete is Economical. *Michigan Contractor and Builder* 100, no. 24 (2006): 16.

Mindess, Sidney, J. Francis Young, and David Darwin. *Concrete*. 2nd ed. Upper Saddle River, NJ: Prentice Hall, (2003).

Purinton Builders Inc. 2010. Web. http://www.purintonbuilders.com/pervious-concrete.aspx

"Route 141 Improvement Project (Ladue to Olive)." N.p., Dec. 2012. Web. http://www.modot.org/stlouis/major_projects/rte141improvementproject.htm.

Shapiro, Mary. "New Stretch of Highway 141 to Open."*Suburban Journals of Greater St. Louis*, July 11, 2012.

"The Metropolitan St. Louis Sewer District: Rules and Regulations and Engineering Design Requirements for Sanitary Sewer and Stormwater Drainage Facility." (2006): 42-86.

Tompkins, Derek, Lev Khazanovich, Michael Darter and Walter Fleischer. "Design and Construction of Sustainable Pavements: Austrian and German Two-Layer Concrete Pavements." *Transportation Research Record: Journal of the Transportation Research Board* no. 2098 (2009): 75-85.

U.S. Department of Transportation. Federal Highway Administration. *Urban Drainage Design Manual Hydraulic Engineering Circular 22, Second Edition*. (2001). Open-file report, U.S. Geological Survey. Washington, DC.

Zhang, Tian, Rao Surampalli, and Keith Lai. Nanotechnostructured Catalysts TiO2 Nanoparticles for Water Purification. *Nanotechnologies for Water Environment Applications.* ed. Tian Zhang, (2009) 43-92. Reston, VA: American Society of Civil Engineers.

VITA

Feras Mohammed El-Ghussein was born on February 22, 1990, in Dubai in the United Arab Emirates. Originally, Mr. El-Ghussein was a Palestinian from the Gaza Strip. He moved to Kansas City along with his family in 1997, and received the majority of his education in public schools in Kansas City, Missouri. He received a Bachelor of Science in Civil Engineering in 2010 from the University of Missouri-Kansas City. He was a member of the civil engineering honors society, Chi Epsilon.

Mr. El-Ghussein had worked in an environmental engineering position for one year after receiving his undergraduate degree. He then returned to receive a Master of Science in Civil Engineering, with an emphasis in Materials Engineering from the University of Missouri-Kansas City.

Mr. El-Ghussein is a member of the American Society of Civil Engineers, American Concrete Institute, and the American Public Works Association.